

**Manuscript version: Author's Accepted Manuscript**

The version presented in WRAP is the author's accepted manuscript and may differ from the published version or Version of Record.

**Persistent WRAP URL:**

<http://wrap.warwick.ac.uk/152347>

**How to cite:**

Please refer to published version for the most recent bibliographic citation information. If a published version is known of, the repository item page linked to above, will contain details on accessing it.

**Copyright and reuse:**

The Warwick Research Archive Portal (WRAP) makes this work by researchers of the University of Warwick available open access under the following conditions.

Copyright © and all moral rights to the version of the paper presented here belong to the individual author(s) and/or other copyright owners. To the extent reasonable and practicable the material made available in WRAP has been checked for eligibility before being made available.

Copies of full items can be used for personal research or study, educational, or not-for-profit purposes without prior permission or charge. Provided that the authors, title and full bibliographic details are credited, a hyperlink and/or URL is given for the original metadata page and the content is not changed in any way.

**Publisher's statement:**

Please refer to the repository item page, publisher's statement section, for further information.

For more information, please contact the WRAP Team at: [wrap@warwick.ac.uk](mailto:wrap@warwick.ac.uk).

1     **A novel ATP dependent dimethylsulfoniopropionate lyase in bacteria**  
2                     **that releases dimethyl sulfide and acryloyl-CoA**

3     Chun-Yang Li<sup>1,2†</sup>, Xiu-Juan Wang<sup>1†</sup>, Xiu-Lan Chen<sup>1,3</sup>, Qi Sheng<sup>1</sup>, Shan Zhang<sup>1</sup>, Peng  
4     Wang<sup>2</sup>, Mussa Quareshy<sup>4</sup>, Branko Rihtman<sup>4</sup>, Xuan Shao<sup>1</sup>, Chao Gao<sup>1</sup>, Fuchuan Li<sup>5</sup>,  
5     Shengying Li<sup>1</sup>, Weipeng Zhang<sup>2</sup>, Xiao-Hua Zhang<sup>2</sup>, Gui-Peng Yang<sup>6</sup>, Jonathan D.  
6     Todd<sup>7</sup>, Yin Chen<sup>2,4</sup>, Yu-Zhong Zhang<sup>2,3,8\*</sup>

7  
8     <sup>1</sup>State Key Laboratory of Microbial Technology, Shandong University, Qingdao, China

9     <sup>2</sup>College of Marine Life Sciences, and Frontiers Science Center for Deep Ocean Multispheres  
10    and Earth System, Ocean University of China, Qingdao, China

11    <sup>3</sup>Laboratory for Marine Biology and Biotechnology, Pilot National Laboratory for Marine  
12    Science and Technology, Qingdao, China

13    <sup>4</sup>School of Life Sciences, University of Warwick, Coventry, CV4 7AL, United Kingdom

14    <sup>5</sup>National Glycoengineering Research Center and Shandong Key Laboratory of Carbohydrate  
15    Chemistry and Glycobiology, Shandong University, Qingdao, China.

16    <sup>6</sup>Frontiers Science Center for Deep Ocean Multispheres and Earth System, Key Laboratory of  
17    Marine Chemistry Theory and Technology, Ministry of Education, Ocean University of China,  
18    Qingdao, China.

19    <sup>7</sup>School of Biological Sciences, University of East Anglia, Norwich Research Park, Norwich,  
20    UK.

21    <sup>8</sup>Marine Biotechnology Research Center, State Key Laboratory of Microbial Technology,  
22    Shandong University, Qingdao, China

23

24    † Chun-Yang Li and Xiu-Juan Wang contributed equally to this work.

25    \*Corresponding author: Yu-Zhong Zhang, zhangyz@sdu.edu.cn

## Abstract

Dimethylsulfoniopropionate (DMSP) is an abundant and ubiquitous organosulfur molecule in marine environments with important roles in global sulfur and nutrient cycling. Diverse DMSP lyases in some algae, bacteria and fungi cleave DMSP to yield gaseous dimethyl sulfide (DMS), an infochemical with important roles in atmospheric chemistry. Here we identified a novel ATP-dependent DMSP lyase, DddX. DddX belongs to the acyl-CoA synthetase superfamily and is distinct from the eight other known DMSP lyases. DddX catalyses the conversion of DMSP to DMS via a two-step reaction: the ligation of DMSP with CoA to form the intermediate DMSP-CoA, which is then cleaved to DMS and acryloyl-CoA. The novel catalytic mechanism was elucidated by structural and biochemical analyses. DddX is found in several Alphaproteobacteria, Gammaproteobacteria and Firmicutes, suggesting that this new DMSP lyase may play an overlooked role in DMSP/DMS cycles.

## Main

The organosulfur molecule dimethylsulfoniopropionate (DMSP) is produced in massive amounts by many marine phytoplankton, macroalgae, angiosperms, bacteria and animals (*Curson et al., 2018; Stefels, 2000; Otte et al., 2004; Curson et al., 2017; Raina et al., 2013*). DMSP can function as an antioxidant, osmoprotectant, predator deterrent, cryoprotectant, protectant against hydrostatic pressure, chemoattractant and may enhance the production of quorum sensing molecules (*Sunda et al., 2002; Cosquer et al., 1999; Wolfe et al., 1997; Karsten et al., 1996; Zheng et al., 2020; Seymour et al., 2010; Johnson et al., 2016*). DMSP also has important roles in global sulfur and nutrient cycling (*Kiene et al., 2000; Charlson et al., 1987*). Environmental DMSP can be taken up and catabolised as a carbon and/or sulfur source by diverse microbes, particularly bacteria (*Curson et al., 2011b*). DMSP catabolism can release volatile dimethyl sulfide (DMS) and/or methanethiol (MeSH) (*Reisch et al., 2011a*). DMS is a potent foraging cue for diverse organisms (*Nevitt, 2011*) and the primary biological source of sulfur transferred from oceans to the atmosphere (*Andreae, 1990*), which may participate in the formation of cloud condensation nuclei, and influence the global climate (*Vallina et al., 2007*).

Bacteria can metabolize DMSP via three known pathways, the demethylation pathway (*Howard et al., 2006*), the recently reported oxidation pathway (*Thume et al., 2018*), and the lysis pathway (*Curson et al., 2011b*) (*Figure 1*). The nomenclature of these pathways is based on the reaction type of the enzyme catalyzing the first step of DMSP catabolism. In the demethylation pathway, DMSP demethylase DmdA first

demethylates DMSP to produce methylmercaptopropionate (MMPA) (*Howard et al., 2006*), which can be further catabolized to MeSH and acetaldehyde (*Figure 1*) (*Reisch et al., 2011b; Bullock et al., 2017; Shao et al., 2019*). In the oxidation pathway, DMSP is oxidized to dimethylsulfoxonium propionate (DMSOP), which is further metabolized to dimethylsulfoxide (DMSO) and acrylate; however, enzymes involved in this pathway are unknown (*Thume et al., 2018*) (*Figure 1*).

In the lysis pathway, diverse lyases cleave DMSP to produce DMS and acrylate or 3-hydroxypropionate-CoA (3-HP-CoA), which are further metabolized by ancillary enzymes (*Curson et al., 2011b; Johnston et al., 2016*) (*Figure 1*). There is large biodiversity in DMSP lysis, with eight different known DMSP lyases that encompass four distinct protein families (DddD a CoA-transferase; DddP a metallopeptidase; cupin containing DddL, DddQ, DddW, DddK and DddY; and Alma1 an aspartate racemase) functioning in diverse marine bacteria, algae and fungi (*Figure 1*) (*Curson et al., 2011b; Johnston et al., 2016*). With the exception of DddD, which catalyzes an acetyl-CoA-dependent CoA transfer reaction, all other DMSP lyases directly cleave DMSP (*Bullock et al., 2017; Todd et al., 2007; Alcolombri et al., 2014; Lei et al., 2018*). Recently, several bacterial isolates were reported to produce DMS from DMSP but lack known DMSP lyases in their genomes (*Liu et al., 2018; Zhang et al., 2019*), suggesting the presence of novel enzyme(s) for DMSP degradation in nature.

A common feature of previously characterized DMSP metabolic pathways is that the metabolites (*i.e.* MMPA, acrylate) need to be ligated with CoA for further catabolism (*Figure 1*) (*Curson et al., 2011b; Reisch et al., 2011b*). Currently there is

no known pathway whereby DMSP is ligated with free CoA, and it is tempting to speculate that there may be such a novel DMSP metabolic pathway. In this study, we screened DMSP-catabolizing bacteria from Antarctic samples, and obtained a strain *Psychrobacter* sp. D2 that grew on DMSP and produced DMS. Genetic and biochemical work showed that *Psychrobacter* sp. D2 possesses a novel DMSP lyase termed DddX for DMSP catabolism (**Figure 1**). DddX is an ATP-dependent DMSP lyase which catalyzes a two-step reaction: the ligation of DMSP and CoA, and the cleavage of DMSP-CoA to produce DMS and acryloyl-CoA. We further solved the crystal structure of DddX and elucidated the molecular mechanism for its catalysis based on structural and biochemical analyses. DddX is found in both Gram-negative and Gram-positive bacteria. Our results provide novel insights into the microbial metabolism of DMSP by this novel enzyme.

## **Results**

### **A potentially novel DMSP lyase in a conventional DMSP catabolic gene cluster**

Using DMSP (5 mM) as the sole carbon source, DMSP-catabolizing bacteria were isolated from five Antarctic samples including alga, sediments and seawaters (**Figure 2-figure supplement 1, Supplementary file 1a**). In total, 175 bacterial strains were obtained (**Figure 2-figure supplement 1B**). Among these bacterial strains, *Psychrobacter* sp. D2, a marine gammaproteobacterium, grew well in the medium containing DMSP as the sole carbon source, but not acrylate (**Figure 2A**). Moreover,

gas chromatography (GC) analysis showed that *Psychrobacter* sp. D2 could catabolize DMSP and produce DMS ( $44.8 \pm 1.8$  nmol DMS min<sup>-1</sup> mg protein<sup>-1</sup>) (**Figure 2B**).

To identify the genes involved in DMSP degradation in *Psychrobacter* sp. D2, we sequenced its genome and searched homologs of known DMSP lyases. However, no homologs of known DMSP lyases with amino acid sequence identity higher than 30% were found in its genome (**Supplementary file 1b**), implying that this strain may possess a novel enzyme or a novel pathway for DMSP catabolism. We then sequenced the transcriptomes of this strain when grown with and without DMSP as the sole carbon source. Transcriptional data analyses showed that the transcripts of 4 genes (1696, 1697, 1698 and 1699) that compose a gene cluster were all highly upregulated (**Figure 2-figure supplement 2**) when DMSP was supplied as the sole carbon source, which was further confirmed by RT-qPCR analysis (**Figure 2C**). These results suggest that this gene cluster may participate in DMSP catabolism within *Psychrobacter* sp. D2.

In the gene cluster, 1696 is annotated as a betaine-carnitine-choline transporter (BCCT), sharing 32% amino acid identity with DddT, the predicted DMSP transporter in *Marinomonas* sp. MWYL1 (**Sun et al., 2012; Todd et al., 2007**); 1697 is annotated as an acetate-CoA ligase, and shares 26% sequence identity with the acetyl-CoA synthetase (ACS) in *Giardia lamblia* (**Sánchez et al., 2000**); 1698 is annotated as an aldehyde dehydrogenase, sharing 72% sequence identity with DddC in *Marinomonas* sp. MWYL1 (**Todd et al., 2007**); and 1699 is annotated as an alcohol dehydrogenase, sharing 65% sequence identity with DddB in *Marinomonas* sp. MWYL1 (**Todd et al., 2007**). DddT, DddC and DddB have been reported to be involved in DMSP import

and catabolism (*Sun et al., 2012; Todd et al., 2007; Todd et al., 2010*). The pattern of the identified gene cluster *1696-1699* in *Psychrobacter* sp. D2 is similar to the patterns of those DMSP-catabolizing clusters reported in *Pseudomonas*, *Marinomonas* and *Halomonas*, in which *dddT*, *dddB* and *dddC* are clustered with the DMSP lyase gene *dddD*, but which is missing in *1696-1699* and is replaced by *1697* (*Todd et al., 2007; Todd et al., 2010; Curson et al., 2010*) (*Figure 2D*). These data further support that the *1696-1699* gene cluster is involved in *Psychrobacter* sp. D2 DMSP catabolism and *1697* encodes a DMSP lyase equivalent to DddD. However, the sequence identity between *1697* and DddD is less than 15%, suggesting that *1697* is unlikely a DddD homolog. With these data we predicted that *1697* encodes a novel DMSP lyase in *Psychrobacter* sp. D2, which we term as DddX hereafter.

### **The essential role of DddX in DMSP degradation in *Psychrobacter* sp. D2**

To identify the possible function of *dddX* in DMSP catabolism, we first deleted the majority of the *dddX* gene within the *Psychrobacter* sp. D2 genome to generate a  $\Delta$ *dddX* mutant strain (*Figure 2-figure supplement 3*). The  $\Delta$ *dddX* mutant was unable to grow on DMSP as the sole carbon source, but its ability to utilize DMSP was fully restored to wild type levels by cloned of *dddX* (in pBBR1MCS-*dddX*) (*Figure 3A*), indicating that *dddX* is essential for strain D2 to utilize DMSP. Furthermore, the  $\Delta$ *dddX* mutant lost DMSP lyase activity, *i.e.* it no longer produced DMS when cultured in marine broth 2216 medium with DMSP. DMSP lyase activity was fully restored to wild type levels in the complemented strain ( $\Delta$ *dddX*/pBBR1MCS-*dddX*)

(**Figure 3B**), indicating that *dddX* encodes a functional DMSP lyase enzyme degrading DMSP to DMS.

### **DddX is an ATP-dependent DMSP lyase and its kinetic analysis**

To verify the enzymatic activity of DddX on DMSP, we cloned the *dddX* gene, overexpressed it in *Escherichia coli* BL21 (DE3), and purified the recombinant DddX (**Figure 3-figure supplement 1**). Sequence analysis suggests that DddX is an acetate-CoA ligase, which belongs to the acyl-CoA synthetase (ACD) superfamily and requires CoA and ATP as co-substrates for catalysis (*Musfeldt et al., 2002; Mai et al., 1996*). Thus, we added CoA and ATP into the reaction system when measuring the enzymatic activity of the recombinant DddX on DMSP. GC analysis showed that the recombinant DddX directly acted on DMSP and produce DMS (**Figure 3C**). HPLC analysis uncovered ADP and an unknown product as DMS co-products (**Figure 3D**). The chromatographic retention time of the unknown product was consistent with it being acryloyl-CoA (*Wang et al., 2017; Cao et al., 2017*). Indeed, liquid chromatography-mass spectrometry (LC-MS) analysis found the molecular weight (MW) of the unknown product to be 822.1317, exactly matching acryloyl-CoA (**Figure 3E**). These data demonstrate that DddX is a functional ATP-dependent DMSP lyase that can catalyze DMSP degradation to DMS and acryloyl-CoA.

The biochemical results above suggest that DddX catalyzes a two-step degradation of DMSP, a CoA ligation reaction and a cleavage reaction. To perform this two-step reaction, there are two alternative pathways: (i), DMSP is first cleaved to

form DMS and acrylate, and subsequently CoA is ligated with acrylate (**Figure 3-figure supplement 2A**). In this case, the intermediate acrylate is produced. (ii), CoA is primarily ligated with DMSP to form DMSP-CoA. Then, DMSP-CoA is cleaved, producing DMS and acryloyl-CoA (**Figure 3-figure supplement 2B**). In this scenario, the intermediate DMSP-CoA is produced. To determine the catalytic process of DddX, we monitored the occurrence of acrylate and/or DMSP-CoA in the reaction system via LC-MS. While acrylate was not detectable in the reaction system, a small peak of DMSP-CoA emerged after a 2-min reaction (**Figure 3F**), indicating that DMSP-CoA is primarily formed in the catalytic reaction of DddX, which is then cleaved to generate DMS and acryloyl-CoA.

Knowing the DddX enzyme activity, we examined its *in vitro* properties. The DddX enzyme had an optimal temperature and pH of 40°C and 8.5, respectively (**Figure 3-figure supplement 3A and B**). The apparent  $K_M$  of DddX for ATP and CoA was 2.5 mM (**Figure 3-figure supplement 3C**) and 0.4 mM (**Figure 3-figure supplement 3D**), respectively. DddX had an apparent  $K_M$  value of 0.4 mM for DMSP (**Figure 3-figure supplement 3E**), which is lower than that of most other reported DMSP lyases and the DMSP demethylase DmdA (**Supplementary file 1c**). The  $k_{cat}$  of DddX for DMSP was  $0.7\text{ s}^{-1}$ , with an apparent  $k_{cat}/K_M$  of  $1.6 \times 10^3\text{ M}^{-1}\text{ s}^{-1}$ . The catalytic efficiency of DddX towards DMSP is higher than known DMSP lyases DddK, DddP, DddD, but lower than DddY and Alma1 (**Supplementary file 1c**).

Despite DddX belongs to the ACD superfamily, the amino acid identity between DddX and known ACD enzymes is relatively low, with the highest being 26%

between DddX and the *Giardia lamblia* ACS (*Sánchez et al., 2000*). The  $k_{cat}/K_M$  value of DddX towards DMSP is lower than several reported ACS enzymes towards acetate (*Chan et al., 2011; You et al., 2017*). Because ACS enzymes were reported to have promiscuous activity toward different short chain fatty acids, such as acetate and propionate (*Patel et al., 1987*), we tested the substrate specificity of DddX. The recombinant DddX exhibited no activity towards acetate or propionate (**Figure 3-figure supplement 4**), and the presence of acetate or propionate had little effects on the enzymatic activity of DddX towards DMSP (**Figure 3-figure supplement 5**), indicating that DddX cannot utilize acetate or propionate as a substrate. Furthermore, we tested the ability of the strain D2 to grow with acetate or propionate as the sole carbon source. The wild-type strain D2 could use acetate or propionate as sole carbon source but deletion of *dddX* has little effect on the growth of strain D2 on these substrates (**Figure 3-figure supplement 6**), suggesting that *dddX* is unlikely to be involved in acetate and propionate catabolism. Together, these results indicate that DddX does not function as an acetate-CoA ligase.

### **The crystal structure and the catalytic mechanism of DddX**

To elucidate the structural basis of DddX catalysis, we solved the crystal structure of DddX in complex with ATP by the single-wavelength anomalous dispersion method using a selenomethionine derivative (Se-derivative) (**Supplementary file 1d**). Although there are four DddX monomers arranged as a tetramer in an asymmetric unit (**Figure 4-figure supplement 1A**), gel filtration analysis indicated that DddX

maintains a dimer in solution (*Figure 4-figure supplement 1B*). Each DddX monomer contains a CoA-binding domain and an ATP-grasp domain (*Figure 4A*), with one loop (Gly280-Tyr300) of the CoA-binding domain inserting into the ATP-grasp domain. ATP is bound in DddX mainly via hydrophilic interactions, including hydrogen bonds and salt bridges (*Figure 4B*). The overall structure of DddX is similar to that of NDP-forming acetyl-CoA synthetase ACD1 (*Weiß et al., 2016*) (*Figure 4-figure supplement 2*), with a root mean square deviation (RMSD) between these two structures of 4.6 Å over 581 C<sub>α</sub> atoms. ACD1 consists of separate α- and β-subunits (*Weiß et al., 2016*), which corresponds to the CoA-binding domain and the ATP-grasp domain of DddX, respectively.

Both DddX and ACS belong to the ACD superfamily, which also contains the well-studied ATP citrate lyases (ACLY) (*Weiß et al., 2016; Verschueren et al., 2019; Hu et al., 2017*). The biochemistry of DddX catalysis is similar to that of ACLY, which converts citrate to acetyl-CoA and oxaloacetate with ATP and CoA as co-substrates (*Verschueren et al., 2019; Hu et al., 2017*). The catalytic processes of enzymes in the ACD superfamily involve a conformational change of a “swinging loop” or “phosphohistidine segment”, in which a conserved histidine is phosphorylated (*Weiß et al., 2016; Verschueren et al., 2019; Hu et al., 2017*). Sequence alignment indicated that His292 of DddX is likely the conserved histidine residue to be phosphorylated, and Gly280-Tyr300 is likely the “swinging loop” (*Figure 4-figure supplement 3*). In the crystal structure of DddX, His292 from loop Gly280-Tyr300 directly forms a hydrogen bond with the γ-phosphate of ATP (*Figure*

**4B**), suggesting a potential for phosphorylation, which is further supported by mutational analysis. Mutation of His292 to alanine abolished the activity of DddX (**Figure 4C**), indicating the key role of His292 during catalysis. Circular-dichroism (CD) spectroscopy analysis showed that the secondary structure of His292Ala exhibits little deviation from that of wild-type (WT) DddX (**Figure 4-figure supplement 4**), indicating that the enzymatic activity loss was caused by amino acid replacement rather than by structural change. Altogether, these data suggest that His292 is phosphorylated in the catalysis of DddX on DMSP.

Having solved the crystal structure of the DddX-ATP complex, we next sought to determine the crystal structures of DddX in complex with CoA and DMSP. However, the diffractions of these crystals were poor and all attempts to solve the structures failed. Thus, we docked DMSP and CoA into the structure of DddX. In the docked structure, the CoA molecule is bound in the CoA-binding domain, while the DMSP molecule is bound in the interface between two DddX monomers (**Figure 4-figure supplement 5A**). Because our biochemical results demonstrated that DMSP-CoA is an intermediate of DddX catalysis (**Figure 3F**), we further docked DMSP-CoA into DddX. DMSP-CoA also locates between two DddX monomers (**Figure 4-figure supplement 5B**), and two aromatic residues (Trp391 and Phe435) form cation- $\pi$  interactions with the sulfonium group of DMSP-CoA (**Figure 4-figure supplement 5C**). Mutations of these two residues significantly decreased the enzymatic activities of DddX (**Figure 4C**), suggesting that these residues play important roles in DddX catalysis. To cleave DMSP-CoA into DMS and acryloyl-CoA, a catalytic base is

necessary to deprotonate DMSP-CoA. Structure analysis showed that Tyr181, Asp208 and Glu432 are close to the DMSP moiety (**Figure 4D**) and may function as the general base. Mutational analysis showed that the mutation of Glu432 to alanine abolished the enzymatic activity of DddX, while mutants Tyr181Ala and Asp208Ala still maintained ~40% activities (**Figure 4C**), indicating that Glu432 is the most probable catalytic residue for the final cleavage of DMSP-CoA. CD spectra of these mutants were indistinguishable from that of WT DddX (**Figure 4-figure supplement 4**), suggesting that the decrease in the enzymatic activities of the mutants were caused by residue replacement rather than structural alteration of the enzyme.

Based on structural and mutational analyses of DddX, and the reported molecular mechanisms of the ACD superfamily (*Weiß et al., 2016; Verschueren et al., 2019; Hu et al., 2017*), we proposed the molecular mechanism of DddX catalysis on DMSP (**Figure 5**). Firstly, His292 is phosphorylated by ATP, forming phosphohistidine (**Figure 5A**), which will be brought to the CoA-binding domain through the conformational change of the swinging loop Gly280-Tyr300. Next, the phosphoryl group is most likely transferred to DMSP to generate DMSP-phosphate (**Figure 5B**), which is subsequently attacked by CoA to form DMSP-CoA intermediate (**Figure 5C**). The last step is the cleavage of DMSP-CoA probably initiated by the base-catalyzed deprotonation of Glu432 (**Figure 5D**). Finally, acryloyl-CoA and DMS are generated (**Figure 5E**) and released from the catalytic pocket of DddX.

## **Distribution of DddX in bacteria**

We next set out to determine the diversity and distribution of DddX in bacteria with sequenced genomes. We searched the NCBI Reference Sequence Database using the DddX sequence of *Psychrobacter* sp. D2 as the query. The data presented in **Figure 6** showed that DddX homologs are present in several diverse groups of bacteria, including Alphaproteobacteria, Gammaproteobacteria and Firmicutes. Multiple sequence alignment showed the presence of the key residues involved in phosphorylation (H292), co-ordination of the substrate (e.g. W391) and catalysis (D432), suggesting that these DddX homologs are likely functional in bacterial DMSP catabolism. To further validate that these DddX homologs are indeed functional DMSP degrading enzymes, we chemically synthesized representative *dddX* sequences from Alphaproteobacteria (*Pelagicola* sp. LXJ1103), Gammaproteobacteria (*Psychrobacter* sp. P11G5; *Marinobacterium jannaschii*) and Firmicutes (*Sporosarcina* sp. P33). These candidate DddX enzymes were purified and all were shown to degrade DMSP and produce acryloyl-CoA confirming their predicted activity (**Figure 6-figure supplement 1**). We predict that bacteria containing DddX will have DMSP lyase activity, but this will depend on the expression of this enzyme in the host and substrate availability.

## Discussion

The cleavage of DMSP to produce DMS is a globally important biogeochemical reaction. Although all known DMSP lyases liberate DMS, they belong to different families, and likely evolved independently (**Bullock et al., 2017**). DddD belongs to

the type III acyl CoA transferase family (*Todd et al., 2007*), DddP to the M24 metallopeptidase family enzyme (*Todd et al., 2009*), DddL/Q/W/K/Y to the cupin superfamily enzymes (*Lei et al., 2018; Li et al., 2017*) and Alma1 to the aspartate racemase superfamily (*Alcolombri et al., 2015*). To the best of our knowledge, DddX represents the first DMSP lyase of the ACD superfamily.

Of the reported DMSP lyases, only DddD catalyzes a two-step reaction which comprises a CoA transfer reaction and a cleavage reaction (*Alcolombri et al., 2014*). It is deduced that DMSP-CoA will be generated in the catalytic process of DddD (*Alcolombri et al., 2014; Curson et al., 2011b; Todd et al., 2007*). Despite this similarity, DddX is fundamentally different to DddD. Firstly, the co-substrates of DddX and DddD are different. ATP and CoA are essential co-substrates for the enzymatic activity of DddX, while for DddD catalysis, acetyl-CoA is used as a CoA donor, and ATP is not required (*Johnston et al., 2016; Alcolombri et al., 2014*). When CoA was replaced by acetyl-CoA in the reaction system, DddX failed to catalyze the cleavage of DMSP (*Figure 1-figure supplement 1*). Secondly, the products of DddD and DddX are different. DddD converts DMSP to DMS and 3-HP-CoA, whereas DddX produces DMS and acryloyl-CoA from DMSP. Except for DddD and DddX, all the other DMSP lyases cleave DMSP to DMS and acrylate.

It has been reported that accumulation of acryloyl-CoA is toxic to bacteria (*Reisch et al., 2013; Wang et al., 2017; Cao et al., 2017; Todd et al., 2012*). Thus, *Psychrobacter* sp. D2 requires an efficient system to metabolize the acryloyl-CoA produced from DMSP lysis by DddX. With the transcription of genes *1698* and *1699*,

directly downstream of *dddX* and likely co-transcribed with *dddX*, being significantly enhanced by growth on DMSP, their enzyme products (DddC and DddB) likely participate in the metabolism and detoxification of acryloyl-CoA or downstream metabolites. However, the recombinant 1698 and 1699 exhibited no enzymatic activity on acryloyl-CoA.

The *Psychrobacter* sp. D2 genome also contains *acul* and *acuH* homologs (2674, 0105, 1810, 1692 and 1695) (**Supplementary file 1e**), which may directly act on acryloyl-CoA to produce propionate-CoA or 3-HP-CoA (**Reisch et al., 2013; Wang et al., 2017; Cao et al., 2017; Todd et al., 2012**). If *Psychrobacter* sp. D2 employs its AcuH homolog to convert acryloyl-CoA to 3-HP-CoA (**Cao et al., 2017**), then, given the high sequence identity of 1698 to DddC and 1699 to DddB, it is possible that these enzymes further catabolize 3-HP-CoA to acetyl-CoA (**Alcolombri et al., 2014; Curson et al., 2011b**). Furthermore, we showed that the recombinant 0105, an AcuI homolog, could act on acryloyl-CoA to produce propionate-CoA with NADPH as a cofactor (**Figure 1-figure supplement 2**). Thus, *Psychrobacter* sp. D2 may also employ an AcuI (*i.e.* 0105) to convert acryloyl-CoA to propionate-CoA (**Figure 1**), which would be metabolized through the methylmalonyl-CoA pathway (**Reisch et al., 2013**).

Several DMSP catabolizing bacteria, e.g. *Halomonas* HTNK1 with DddD, are reported to utilize acrylate as the carbon source for growth via e.g. *acuN*, *acuK*, *acuI*, *acuH* and *prpE* gene products (**Curson et al., 2011a; Reisch et al., 2013; Todd et al., 2010**). Despite the presence of several *acuN*, *acuK*, *acuI*, *acuH* and *prpE* homologs in

its genome (**Supplementary file 1e**), *Psychrobacter* sp. D2 could not use acrylate as a sole carbon source (**Figure 2A**). Thus, *Psychrobacter* sp. D2 either (i), lacks a functional acrylate transporter; (ii), these homologs that are predicted to be involved in acrylate metabolism are not functional *in vivo*; or (iii), these genes are not induced by acrylate. Clearly further biochemical and genetic experiments are required to establish the how acryloyl-CoA is catabolized in this bacterium.

Many marine bacteria, especially roseobacters, are reported to metabolize DMSP via more than one pathway (**Curson et al., 2011b; Bullock et al., 2017**). For example, *Ruegeria pomeroyi* DSS-3, one of the type strains of the marine *Roseobacter* clade, possesses both the demethylation and the lysis pathway for DMSP metabolism (**Reisch et al., 2013**). Moreover, it contains multiple *ddd* genes (*dddQ*, *dddP* and *dddW*) (**Reisch et al., 2013; Todd et al., 2011**). DmdA homologs were not identified in the genome of *Psychrobacter* sp. D2, indicating that the demethylation pathway is absent in strain D2. The fact that the mutant  $\Delta dddX$  could not produce DMS from DMSP and was unable to grow on DMSP as the sole carbon source suggests that *Psychrobacter* sp. D2 only possesses one DMSP lysis pathway for DMSP degradation. Why some bacteria have evolved multiple DMSP utilization pathways and some bacteria only possess one pathway awaits further investigation.

Here, we demonstrate that DddX is a functional DMSP lyase present in several isolates of Gammaproteobacteria, Alphaproteobacteria and, notably, Gram-positive Firmicutes, e.g. in *Sporosarcina* sp. P33. The distribution of DddX in these bacterial lineages points to the role of horizontal gene transfer (HGT) in the dissemination of

*dddX* in environmental bacteria and this certainly warrants further investigation. Interestingly, DddX is found in several bacterial isolates which were isolated from soil or plant roots, suggesting that DMSP may also be produced in these ecosystems. Finally, it has been reported that many other Gram-positive actinobacteria can make DMS from DMSP (*Liu et al., 2018*). Interestingly, these Actinobacteria lack *dddX* and any other known DMSP lyase genes. Thus, there is still more biodiversity in microbial DMSP lyases to be uncovered.

## **Conclusion**

DMSP is widespread in nature and cleavage of DMSP produces DMS, an important mediator in the global sulfur cycle. In this study, we report the identification of a novel ATP-dependent DMSP lyase DddX from marine bacteria. DddX belongs to the ACD superfamily, and catalyzes the conversion of DMSP to DMS and acryloyl-CoA, with CoA and ATP as co-substrates. DddX homologs are found in both Gram-positive and Gram-negative bacterial lineages. This study offers new insights into how diverse bacteria cleave DMSP to generate the climatically important gas DMS.

## Key Resources Table

Reagent type (species) or resource	Designation	Source or reference	Identifiers	Additional information
Strain, strain background ( <i>Psychrobacter</i> <i>sp.</i> )	D2	This study; Zhang Laboratory		Wild-type isolate; Available from Zhang lab
Strain, strain background ( <i>Psychrobacter</i> <i>sp.</i> )	$\Delta dddX$	This study; Zhang Laboratory		the <i>dddX</i> gene deletion mutant of <i>Psychrobacter</i> <i>sp.</i> D2; Available from Zhang lab
Strain, strain background ( <i>Psychrobacter</i> <i>sp.</i> )	$\Delta dddX$ /pBBR1 MCS- <i>dddX</i>	This study; Zhang Laboratory		$\Delta dddX$ containing pBBR1MCS- <i>d</i> <i>dddX</i> plasmid; Available from Zhang lab
Strain, strain background ( <i>Psychrobacter</i> <i>sp.</i> )	$\Delta dddX$ /pBBR1 MCS	This study; Zhang Laboratory		$\Delta dddX$ containing pBBR1MCS plasmid; Available from Zhang lab
Strain, strain background ( <i>Escherichia</i> . <i>coli</i> )	WM3064	<i>Dehio et al., 1997</i>		Conjugation donor strain
Strain, strain background ( <i>Escherichia</i> . <i>coli</i> )	DH5 $\alpha$	Vazyme Biotech company (China)		Transformed cells for gene cloning

Strain, strain background ( <i>Escherichia. coli</i> )	BL21(DE3)	Vazyme Biotech company (China)	Transformed cells for gene expression
Recombinant DNA reagent	pK18 <i>mobsacB</i> -Ery	<b>Wang et al., 2015</b>	Gene knockout vector
Recombinant DNA reagent	pK18Ery- <i>dddX</i>	This study; Zhang Laboratory	pK18 <i>mobsacB</i> -Ery containing the homologous arms of the <i>dddX</i> gene of <i>Psychrobacter</i> . sp. D2; Available from Zhang lab
Recombinant DNA reagent	pBBR1MCS	<b>Kovach et al., 1995</b>	Broad-host-range cloning vector
Recombinant DNA reagent	pBBR1MCS- <i>ddX</i>	This study; Zhang Laboratory	pBBR1MCS containing the <i>dddX</i> gene and its promoter of <i>Psychrobacter</i> . sp. D2; Available from Zhang lab
Recombinant DNA reagent	pET-22b- <i>dddX</i>	This study; Zhang Laboratory	Used for <i>dddX</i> expression; Available from Zhang lab
Commercial assay or kit	Pierce <sup>TM</sup> BCA Protein Assay Kit	Thermo, USA	Protein assay
Commercial assay or kit	Bacterial genomic DNA isolation kit	BioTeke Corporation, China	DNA extraction

Commercial assay or kit	RNeasy Mini Kit	QIAGEN, America	RNA extraction
Commercial assay or kit	PrimeScript™ RT reagent Kit	Takara, Japan	Reverse transcription
Commercial assay or kit	Genome sequencing of <i>Psychrobacter</i> sp. D2	Biozon Biotechnology Co., Ltd, China	NCBI: JACDXZ 000000000
Commercial assay or kit	Transcriptome sequencing of <i>Psychrobacter</i> sp. D2	BGI Tech Solutions Co., Ltd, China	NCBI: PRJNA646786
Software, algorithm	HKL3000 program	<i>Minor et al., 2006</i>	Diffraction data analysis
Software, algorithm	CCP4 program Phaser	<i>Winn et al., 2011</i>	Diffraction data analysis
Software, algorithm	Coot	<i>Emsley et al., 2010</i>	Diffraction data analysis
Software, algorithm	<i>Phenix</i>	<i>Adams et al., 2010</i>	Diffraction data analysis
Software, algorithm	PyMOL	Schrödinger, LLC	<a href="http://www.py-mol.org/">http://www.py-mol.org/</a>
Software, algorithm	MEGA 7	<i>Kumar et al., 2016</i>	Phylogenetic analysis

388

389 **Bacterial strains, plasmids and growth conditions.** Strains and plasmids used in  
390 this study are shown in *Supplementary file 1f*. Isolates were cultured in the marine  
391 broth 2216 medium or the basal medium (*Supplementary file 1g*) with 5 mM DMSP  
392 as the sole carbon source at 15-25°C. *Psychrobacter* sp. D2 was cultured in the

marine broth 2216 medium or the basal medium (*Supplementary file 1g*) supplied with different carbon sources (sodium pyruvate, acrylate or DMSP at a final concentration of 5 mM) at 15-25°C. The *E. coli* strains DH5 $\alpha$  and BL21(DE3) were grown in the Lysogeny Broth (LB) medium at 37°C. Diaminopimelic acid (0.3 mM) was added to culture the *E. coli* WM3064 strain.

**Isolation of bacterial strains from Antarctic samples.** A total of five samples were collected from the Great Wall Station of Antarctica during the Chinese Antarctic Great Wall Station Expedition in January, 2017. Information of samples is shown in *Figure 2-figure supplement 1 and Supplementary file 1a*. Algae and sediments were collected using a grab sampler and stored in airtight sterile plastic bags at 4°C. Seawater samples were filtered through polycarbonate membranes with 0.22  $\mu$ m pores (Millipore Co., United States). The filtered membranes were stored in sterile tubes (Corning Inc., United States) at 4°C. All samples were transferred into a 50 ml flask containing 20 ml 3% (w/v) seasalt solution (SS) and shaken at 100 rpm at 15°C for 2 h. The suspension obtained was subsequently diluted to 10<sup>-6</sup> with sterile SS. An aliquot (200  $\mu$ l) of each dilution was spread on the basal medium (*Supplementary file 1g*) plates with 5 mM DMSP as the sole carbon source. The plates were then incubated at 15°C in the dark for 2-3 weeks. Colonies with different appearances were picked up and were further purified by streaking on the marine 2216 agar plates for at least three passages. The abilities of the colonies for DMSP catabolism were verified in a liquid basal medium with DMSP (5 mM) as the sole carbon source. The isolates were stored at -80°C in the marine broth 2216 medium containing 20% (v/v) glycerol.

**Sequence analysis of bacterial 16S rRNA genes.** Genomic DNA of the isolates was extracted using a bacterial genomic DNA isolation kit (BioTeke Corporation, China) according to the manufacturer's instructions. The 16S rRNA genes of these strains were amplified using the primers 27F/1492R (*Supplementary file 1h*) and sequenced to determine their taxonomy. Pairwise similarity values for the 16S rRNA gene of the cultivated strains were calculated through the EzBiolcloud server (<http://www.ezbiocloud.net/>) (Yoon *et al.*, 2017).

**Bacterial growth assay with DMSP as the sole carbon source.** Cells were grown in the marine broth 2216 medium, harvested after incubation at 15°C for 24 h, and then washed three times with sterile SS. The washed cells were diluted to the same density of OD<sub>600</sub> ≈ 2.0, and then 1% (v/v) cells were inoculated into the basal medium with DMSP, sodium acetate or sodium propionate (5 mM) as the sole carbon source. The bacteria were cultured in the dark at 15°C. The growth of the bacteria was measured by detecting the OD<sub>600</sub> of the cultures at different time points using a spectrophotometer V-550 (Jasco Corporation, Japan).

**Quantification of DMS by GC.** To measure the production of DMS, cells were first cultured overnight in the marine broth 2216 medium, and then washed three times with sterile SS. The washed cells were diluted to the same density of OD<sub>600</sub> ≈ 0.3, then diluted 1:10 into vials (Anpel, China) containing the basal medium supplied with 5 mM DMSP as the sole carbon source. The vials were crimp sealed with rubber bungs and incubated for 2 h at 25°C. The cultures were then assayed for DMS production on a gas chromatograph (GC-2030, Shimadzu, Japan) equipped with a

flame photometric detector (*Liu et al., 2018*). An eight-point calibration curve of DMS standards was used (*Curson et al., 2017*). Abiotic controls of the basal medium amended with 5 mM DMSP were set up and incubated under the same conditions to monitor the background lysis of DMSP to DMS. Following growth of all bacteria strains in the marine broth 2216 medium, cells were collected by centrifugation, resuspended in the lysis buffer (50 mM Tris-HCl, 100 mM NaCl, 0.5% glycerol, pH 8.0), and lysed by sonicated. The protein content in the cells was measured by Pierce<sup>TM</sup> BCA Protein Assay Kit (Thermo, USA). DMS production is expressed as  $\text{nmol min}^{-1} \text{mg protein}^{-1}$ .

**Transcriptome sequencing of *Psychrobacter* sp. D2.** Cells of strain D2 were cultured in the marine broth 2216 medium at 180 rpm at 15°C for 24 h. The cells were collected and washed three times with sterile SS, and then cultured in sterile SS at 180 rpm at 15°C for 24 h. Subsequently, the cells were washed twice with sterile SS, and incubated at 4°C for 24 h. After incubation, the cells were harvested and resuspended in sterile SS, which were used as the resting cells. The resting cells were inoculated into the basal medium with DMSP (5 mM) as the sole carbon source, and incubated at 180 rpm at 15°C. When the OD<sub>600</sub> of the cultures reached 0.3, the cells were harvested. The resting cells and those cultured in the basal medium with sodium pyruvate (5 mM) as the sole carbon source were set up as controls. Total RNA was extracted using a RNeasy Mini Kit (QIAGEN, America) according to the manufacturer's protocol. After validating the quality, RNA samples were sent to BGI Tech Solutions Co., Ltd (China) for transcriptome sequencing and subsequent

bioinformatic analysis.

**Real-Time qPCR analysis.** Cells of *Psychrobacter* sp. D2 were cultured in the marine broth 2216 medium at 180 rpm at 15°C to an OD<sub>600</sub> of 0.8. Then, cells were induced by 5 mM DMSP, and the control group without DMSP was also set up. After 20 min's induction, total RNA was extracted using a RNeasy Mini Kit (Qiagen, Germany) according to the manufacturer's instructions. Genomic DNA was removed using gDNA Eraser (TaKaRa, Japan) and cDNA was synthesized using a PrimeScript<sup>TM</sup> RT reagent Kit. The qPCR was performed on the Light Cycler II System (Roche, Switzerland) using a SYBR® Premix Ex Taq<sup>TM</sup> (TaKaRa, Japan). Relative expression levels of target genes were calculated using the LightCycler®480 software with the “Advanced Relative Quantification” method. The *recA* gene was used as an internal reference gene. The primers used in this study are shown in *Supplementary file 1h*.

**Genetic manipulations of *Psychrobacter* sp. D2.** Deletion of the *dddX* gene was performed via pK18*mobsacB*-Ery-based homologue recombination (*Wang et al., 2015*). The upstream and downstream homologous sequences of the *dddX* gene were amplified with primer sets *dddX*-UP-F/*dddX*-UP-R and *dddX*-Down-F/*dddX*-Down-R, respectively. Next, the PCR fragments were inserted to the vector pK18*mobsacB*-Ery with *HindIII*/*BamHI* as the restriction sites to generate pK18Ery-*dddX*, which was transferred into *E. coli* WM3064. The plasmid pK18Ery-*dddX* was then mobilized into *Psychrobacter* sp. D2 by intergeneric conjugation with *E. coli* WM3064. To select for colonies in which the pK18Ery-*dddX* had integrated into the *Psychrobacter*

sp. D2 genome by a single crossover event, cells were plated on the marine 2216 agar plates containing erythromycin (25 µg/ml). Subsequently, the resultant mutant was cultured in the marine broth 2216 medium and plated on the marine 2216 agar plates containing 10% (w/v) sucrose to select for colonies in which the second recombination event occurred. Single colonies appeared on the plates were streaked on the marine 2216 agar plates containing erythromycin (25 µg/ml), and colonies sensitive to erythromycin were further validated to be the *dddX* gene deletion mutants by PCR with primer pairs of *dddX*-1000-F/*dddX*-1000-R and *dddX*-300Up-F/*dddX*-700Down-R.

For complementation of the  $\Delta$ *dddX* mutant, the *dddX* gene with its native promoter was amplified using the primers set *dddX*-pBBR1-PF/*dddX*-pBBR1-PR. The PCR fragment was digested with *Kpn*I and *Xho*I, and then inserted into the vector pBBR1MCS to generate pBBR1MCS-*dddX*. This plasmid was then transformed into *E. coli* WM3064, and mobilized into the  $\Delta$ *dddX* mutant by intergeneric conjugation. After mating, the cells were plated on the marine 2216 agar plates containing kanamycin (80 µg/ml) to select for the complemented mutant. The empty vector pBBR1MCS was mobilized into the  $\Delta$ *dddX* mutant using the same protocol. Colony PCR was used to confirm the presence of the transferred plasmid. The strains, plasmids and primers used in this study are shown in *Supplementary file 1f* and *Supplementary file 1h*.

**Gene cloning, point mutation and protein expression and purification.** The 2247 bp full-length *dddX* gene was amplified from the genome of *Psychrobacter* sp. D2 by

PCR using *FastPfu* DNA polymerase (TransGen Biotech, China). The amplified gene was then inserted to the *NdeI/XhoI* restriction sites of the pET-22b vector (Novagen, Germany) with a C-terminal His tag. All of the point mutations in DddX were introduced using the PCR-based method and verified by DNA sequencing. The DddX protein and its mutants were expressed in *E. coli* BL21 (DE3). The cells were cultured in the LB medium with 0.1 mg/ml ampicillin at 37°C to an OD<sub>600</sub> of 0.8-1.0 and then induced at 18°C for 16 h with 0.5 mM isopropyl-β-D-thiogalactopyranoside (IPTG). After induction, cells were collected by centrifugation, resuspended in the lysis buffer (50 mM Tris-HCl, 100 mM NaCl, 0.5% glycerol, pH 8.0), and lysed by pressure crusher. The proteins were first purified by affinity chromatography on a Ni<sup>2+</sup>-NTA column (GE healthcare, America), and then fractionated by anion exchange chromatography on a Source 15Q column (GE healthcare, America) and gel filtration on a Superdex G200 column (GE healthcare, America). The Se-derivative of DddX was overexpressed in *E. coli* BL21 (DE3) under 0.5 mM IPTG induction in the M9 minimal medium supplemented with selenomethionine, lysine, valine, threonine, leucine, isoleucine and phenylalanine. The recombinant Se-derivative was purified using the aforementioned protocol for the wild-type DddX.

**Enzyme assay and product identification.** For the routine enzymatic activity assay of the DddX protein, the purified DddX protein (at a final concentration of 0.1 mM) was incubated with 1 mM DMSP, 1 mM CoA, 1 mM ATP, 2 mM MgCl<sub>2</sub> and 100 mM Tris-HCl (pH 8.0). The reaction was performed at 37°C for 0.5 h, and terminated by adding 10% (v/v) hydrochloric acid. The control groups had the same reaction system

except that the DddX protein was not added. DMS was detected by GC as described above. Products of acryloyl-CoA and DMSP-CoA were analyzed using LC-MS. Components of the reaction system were separated on a reversed-phase SunFire C<sub>18</sub> column (Waters, Ireland) connected to a high performance liquid chromatography (HPLC) system (Dionex, United States). The ultraviolet absorbance of samples was detected by HPLC under 260 nm. The samples were eluted with a linear gradient of 1-20% (v/v) acetonitrile in 50 mM ammonium acetate (pH 5.5) over 24 min. The HPLC system was coupled to an impact HD mass spectrometer (Bruker, Germany) for *m/z* determination. To determine the optimal temperature for DddX enzymatic activity, reaction mixtures containing 5 mM DMSP, 5 mM CoA, 5 mM ATP, 6 mM MgCl<sub>2</sub>, 100 mM Tris-HCl (pH 8.5) and 10 µM DddX were incubated at 5-50°C (with a 5°C interval) for 15 min. The optimum pH for DddX enzymatic activity was examined at 40°C (the optimal temperature for DddX enzymatic activity) using Britton-Robinson Buffer (**Britton, 1952**) with pH from 7.5 to 11.0, with a 0.5 interval. The kinetic parameters of DddX were measured by determining the production of DMS with nonlinear analysis based on the initial rates, and all the measurements were performed at the optimal pH and temperature.

The enzymatic activity of DddX toward sodium acetate or sodium propionate was measured by determining the production of acetyl-CoA or propionyl-CoA using HPLC as described above with DMSP replaced by sodium acetate or sodium propionate. To determine the effects of sodium acetate or sodium propionate on the enzymatic activity of DddX toward DMSP, sodium acetate or sodium propionate at a

final concentration of 1 mM, 2 mM or 5 mM were individually added to the reaction mixture. All the measurements were performed at the optimum pH and temperature for DddX.

The enzymatic activity of 0105 (AclI) toward acryloyl-CoA was measured by determining the production of propionate-CoA using HPLC as described above. The reaction mixture contained 2 mM DMSP, 2 mM CoA, 2 mM ATP, 10 mM MgCl<sub>2</sub>, 1 mM NADPH, 100 mM Tris-HCl (pH 8.5), 0.1 mM DddX and 0.9 mM 0105. The reaction was performed at 40°C, pH 8.5 for 2 h, and terminated by adding 10% (v/v) hydrochloric acid.

**Crystallization and data collection.** The purified DddX protein was concentrated to ~ 8 mg/ml in 10 mM Tris-HCl (pH 8.0) and 100 mM NaCl. The DddX protein was mixed with ATP (1 mM), and the mixtures were incubated at 0°C for 1 h. Initial crystallization trials for DddX/ATP complex were performed at 18°C using the sitting-drop vapor diffusion method. Diffraction-quality crystals of DddX/ATP complex were obtained in hanging drops containing 0.1 M lithium sulfate monohydrate, 0.1 M sodium citrate tribasic dihydrate (pH 5.5) and 20% (w/v) polyethylene glycol (PEG) 1000 at 18°C after 2-week incubation. Crystals of the DddX Se-derivative were obtained in hanging drops containing 0.1 M HEPES (pH 7.5), 10% PEG 6000 and 5% (v/v) (+/-)-2-Methyl-2,4-pentanediol at 18°C after 2-week incubation. X-ray diffraction data were collected on the BL18U1 and BL19U1 beamlines at the Shanghai Synchrotron Radiation Facility. The initial diffraction data sets were processed using the HKL3000 program with its default settings (*Minor et*

569 *al.*, 2006).

570 **Structure determination and refinement.** The crystals of DddX/ATP complex  
571 belong to the C2 space group, and Se-derivative of DddX belong to the  $P2_12_12_1$  space  
572 group. The structure of DddX Se-derivative was determined by single-wavelength  
573 anomalous dispersion phasing. The crystal structure of DddX/ATP complex was  
574 determined by molecular replacement using the CCP4 program Phaser (*Winn et al.*,  
575 2011) with the structure of DddX Se-derivative as the search model. The refinements  
576 of these structures were performed using Coot (*Emsley et al.*, 2010) and Phenix  
577 (*Adams et al.*, 2010). All structure figures were processed using the program PyMOL  
578 (<http://www.pymol.org/>).

579 **Circular dichroism (CD) spectroscopy.** CD spectra for WT DddX and its mutants  
580 were carried out in a 0.1 cm-path length cell on a JASCO J-1500 Spectrometer  
581 (Japan). All proteins were adjusted to a final concentration of 0.2 mg/ml in 10 mM  
582 Tris-HCl (pH 8.0) and 100 mM NaCl. Spectra were recorded from 250 to 200 nm at a  
583 scan speed of 200 nm/min.

584 **Molecular docking simulations.** The structure of the DddX/ATP complex containing  
585 a pair of subunits,  $\alpha$  &  $\beta$  was loaded and energy minimised in Flare (v3.0, Cresset)  
586 involving 11248 moving heavy atoms (Chain A: 5312, Chain B: 5312, Chain G: 10  
587 and Chain S Water: 614). The molecule minimized with 2000 iterations using a  
588 gradient of 0.657 kcal/Å. The minimised structure had an RMSD 0.82Å relative to the  
589 starting structure and a decrease in starting energy from 134999.58 kcal/mol to a final  
590 energy of 6888.60 kcal/mol. The DMSP, CoA and DMSP-CoA molecules were drawn

in MarvinSketch (v19.10.0, 2019, ChemAxon for Mac) and exported as a Mol SDF format. The molecules were imported into Flare and docked into the proposed CoA/DMSP binding site using the software's default docking parameters for intensive pose searching and scoring.

**Identification of DddX homologs in bacteria and phylogenetic analysis.** DddX (1697) of *Psychrobacter* sp. D2 was used as the query sequence to search for homologs in genome-sequenced bacteria in the NCBI Reference Sequence Database (RefSeq, <https://www.ncbi.nlm.nih.gov/refseq/>) using BLASTP with a stringent setting with an e-value cut-off < -75, sequence coverage >70% and percentage identity >30%. These high stringency settings are necessary to exclude other acetyl-CoA synthetase family proteins (ACS) which are unlikely to be involved in DMSP catabolism. Multiple sequence alignment was carried out using MEGA 7 (Kumar *et al.*, 2016) and the presence of histidine 292, tryptophan 391 and glutamate 432 was manually inspected. To confirm the activity of DddX homologs from retrieved sequences from these genome-sequenced bacteria, four sequences (*Sporosarcina* sp. P33; *Psychrobacter* sp. P11G5; *Marinobacterium jannaschii*; *Pelagicola* sp. LXJ1103) were chemically-synthesized and their enzyme activity for DMSP degradation was confirmed experimentally (Figure 6-figure supplement 1). The phylogenetic tree was constructed using the neighbour-joining method with 500 bootstraps using MEGA 7 (Kumar *et al.*, 2016). The characterized ACS ACD1 (Weiße *et al.*, 2016) was used as the outgroup.

**Data and materials availability.** The draft genome sequences of *Psychrobacter* sp.

613 D2 have been deposited in the National Center for Biotechnology Information (NCBI)  
614 Genome database under accession number JACDXZ000000000. All the RNA-seq  
615 read data have been deposited in NCBI's sequence read archive (SRA) under project  
616 accession number PRJNA646786. The structure of DddX/ATP complex has been  
617 deposited in the PDB under the accession code 7CM9.  
618

## References

- Adams PD**, Afonine PV, Bunkóczi G, Chen VB, Davis IW, Echols N, Headd JJ, Hung LW, . Kapral GJ, Grosse-Kunstleve RW, McCoy AJ, . Moriarty NW, Oeffner R, Read RJ, Richardson DC, Richardson JS, Terwilliger TC, Zwart PH. 2010. PHENIX: a comprehensive Python-based system for macromolecular structure solution. *Acta Crystallographica Section D-Biological Crystallography* **66**:213-221. DOI: 10.1107/S0907444909052925, PMID: 20124702
- Alcolombri U**, Ben-Dor S, Feldmesser E, Levin Y, Tawfik DS, Vardi A. 2015. Identification of the algal dimethyl sulfide-releasing enzyme: A missing link in the marine sulfur cycle. *Science* **348**:1466-1469. DOI: 10.1126/science.aab1586, PMID: 26113722
- Alcolombri U**, Laurino P, Lara-Astiaso P, Vardi A, Tawfik DS. 2014. DddD is a CoA-transferase/lyase producing dimethyl sulfide in the marine environment. *Biochemistry* **53**:5473-5475. DOI: 10.1021/bi500853s, PMID: 25140443
- Andreae MO**. 1990. Ocean-atmosphere interactions in the global biogeochemical sulfur cycle. *Marine Chemistry* **30**:1-29. DOI: 10.1016/0304-4203(90)90059-1.
- Britton HT**. 1952. *Hydrogen Ions*, 4th edn. London; Chapman and Hall.
- Brummett AE**, Schnicker NJ, Crider A, Todd JD, Dey M. 2015. Biochemical, kinetic, and spectroscopic characterization of *Ruegeria pomeroyi* DddW-A mononuclear iron-dependent DMSP lyase. *PLOS ONE* **10**:e0127288. DOI: 10.1371/journal.pone.0127288, PMID: 25993446
- Bullock HA**, Luo H, Whitman WB. 2017. Evolution of dimethylsulfoniopropionate metabolism in marine phytoplankton and bacteria. *Frontiers in Microbiology* **8**:637. DOI: 10.3389/fmicb.2017.00637, PMID: 28469605
- Cao HY**, Wang P, Xu F, Li PY, Xie BB, Qin QL, Zhang YZ, Li CY, Chen XL. 2017. Molecular insight into the acryloyl-CoA hydration by AcuH for acrylate detoxification in dimethylsulfoniopropionate-catabolizing bacteria. *Frontiers in Microbiology* **8**:2034. DOI: 10.3389/fmicb.2017.02034, PMID: 29089943
- Chan CH**, Garrity J, Crosby HA, Escalante-Semerena JC. 2011. In *Salmonella enterica*, the sirtuin-dependent protein acylation/deacylation system (SDPADS) maintains energy homeostasis during growth on low concentrations of acetate. *Molecular Microbiology* **80**:168-183. DOI: 10.1111/j.1365-2958.2011.07566.x, PMID: 21306440
- Charlson RJ**, Lovelock JE, Andreae MO, Warren, SG. 1987. Oceanic phytoplankton, atmospheric sulphur, cloud albedo and climate. *Nature* **326**:655-661. DOI: 10.1038/326655a0
- Cosquer A**, Pichereau V, Pocard JA, Minet J, Cormier M, Bernard T. 1999. Nanomolar levels of dimethylsulfoniopropionate, dimethylsulfonioacetate, and glycine betaine are sufficient to confer osmoprotection to *Escherichia coli*. *Applied and Environmental Microbiology* **65**:3304-3311. DOI: 10.1128/AEM.65.8.3304-3311.1999, PMID: 10427011
- Curson ARJ**, Liu J, Martinez AB, Green RT, Chan Y, Carrión O, Williams BT, Zhang SH, Yang GP, Bulman Page PC, Zhang XH, Todd JD. 2017. Dimethylsulfoniopropionate biosynthesis in marine bacteria and identification of the key gene in this process. *Nature Microbiology* **2**:17009. DOI: 10.1038/nmicrobiol.2017.9, PMID: 28191900

- Curson ARJ**, Rogers R, Todd JD, Brearley CA, Johnston AWB. 2008. Molecular genetic analysis of a dimethylsulfoniopropionate lyase that liberates the climate-changing gas dimethylsulfide in several marine alphaproteobacteria and *Rhodobacter sphaeroides*. *Environmental Microbiology* **10**:757 – 767. DOI: 10.1111/j.1462-2920.2007.01499.x, PMID: 18237308
- Curson ARJ**, Sullivan MJ, Todd JD, Johnston AWB. 2010. Identification of genes for dimethyl sulfide production in bacteria in the gut of Atlantic Herring (*Clupea harengus*). *The ISME Journal* **4**:144-146. DOI: 10.1038/ismej.2009.93, PMID: 19710707
- Curson ARJ**, Sullivan MJ, Todd JD, Johnston AWB. 2011a. DddY, a periplasmic dimethylsulfoniopropionate lyase found in taxonomically diverse species of Proteobacteria. *The ISME Journal* **5**:1191-1200. DOI: 10.1038/ismej.2010.203, PMID: 21248856
- Curson ARJ**, Todd JD, Sullivan MJ, Johnston AWB. 2011b. Catabolism of dimethylsulphonioipropionate: microorganisms, enzymes and genes. *Nature Reviews Microbiology* **9**:849-859. DOI: 10.1038/nrmicro2653, PMID: 21986900
- Curson ARJ**, Williams BT, Pinchbeck BJ, Sims LP, Martínez AB, Rivera PPL, Kumaresan D, Mercadé E, Spurgin LG, Carrión O, Moxon S, Cattolico RA, Kuzhiumparambil U, Guagliardo P, Clode PL, Raina JB, Todd JD. 2018. DSYB catalyses the key step of dimethylsulfoniopropionate biosynthesis in many phytoplankton. *Nature Microbiology* **3**:430-439. DOI: 10.1038/s41564-018-0119-5, PMID: 29483657
- de Souza MP**, Yoch DC. 1995. Comparative physiology of dimethyl sulfide production by dimethylsulfoniopropionate lyase in *Pseudomonas doudoroffii* and *Alcaligenes* sp. strain M3A. *Applied and Environmental Microbiology* **61**:3986-3991. DOI: 10.1128/AEM.61.11.3986-3991.1995, PMID: 16535162
- Dehio C**, Meyer M. 1997. Maintenance of broad-host-range incompatibility group P and group Q plasmids and transposition of Tn5 in *Bartonella henselae* following conjugal plasmid transfer from *Escherichia coli*. *Journal of Bacteriology* **179**:538-540. DOI: 10.1128/jb.179.2.538-540.1997, PMID: 8990308
- Emsley P**, Lohkamp B, Scott WG, Cowtan K. 2010. Features and development of Coot. *Acta Crystallographica Section D-Biological Crystallography* **66**:486-501. DOI: 10.1107/S0907444910007493, PMID: 20383002
- Gasteiger E**, Bairoch A, Appel RD. 2005. Protein identification and analysis tools on the ExPASy server. In: Walker JM, editor. *The Proteomics Protocols Handbook*. pp. 571-607. DOI: 10.1385/1-59259-890-0:571
- Howard EC**, Henriksen JR, Buchan A, Reisch CR, Bürgmann H, Welsh R, Ye W, González JM, Mace K, Joye SB, Kiene RP, Whitman WB, Moran MA. 2006. Bacterial taxa that limit sulfur flux from the ocean. *Science* **314**:649-652. DOI: 10.1126/science.1130657, PMID: 17068264
- Hu J**, Komakula A, Fraser ME. 2017. Binding of hydroxycitrate to human ATP-citrate lyase. *Acta Crystallographica Section D-Structural Biology* **73**:660-671. DOI: 10.1107/S2059798317009871, PMID: 28777081
- Johnson WM**, Kido Soule MC, Kujawinski EB. 2016. Evidence for quorum sensing and differential metabolite production by a marine bacterium in response to DMSP. *The ISME Journal* **10**:2304-2316.

DOI: 10.1038/ismej.2016.6, PMID: 26882264

**Johnston AWB**, Green RT, Todd JD. 2016. Enzymatic breakage of dimethylsulfoniopropionate-a signature molecule for life at sea. *Current Opinion in Chemical Biology* **31**:58-65. DOI: 10.1016/j.cbpa.2016.01.011, PMID: 26851513

**Kanagawa T**, Dazai M, Fukuoka S. 1982. Degradation of O,O-Dimethyl phosphorodithioate by *Thiobacillus thioparus* TK-1 and *Pseudomonas* AK-2. *Agricultural and Biological Chemistry* **46**:2571-2578. DOI: 10.1080/00021369.1982.10865475

**Karsten U**, Kück K, Vogt C, Kirst GO. 1996. Dimethylsulfoniopropionate production in phototrophic organisms and its physiological functions as a cryoprotectant. In: Kiene RP, Visscher PT, Keller MD, Kirst GO, editors. *Biological and Environmental Chemistry of DMSP and Related Sulfonium Compounds*. Springer, Boston, MA. pp. 143-153. DOI: 10.1007/978-1-4613-0377-0\_13

**Kiene RP**, Linn LJ, Bruton JA. 2000. New and important roles for DMSP in marine microbial communities. *Journal of Sea Research* **43**:209-224. DOI: 10.1016/S1385-1101(00)00023-X

**Kirkwood M**, Le Brun NE, Todd JD, Johnston AWB. 2010. The *dddP* gene of *Roseovarius nubinhibens* encodes a novel lyase that cleaves dimethylsulfoniopropionate into acrylate plus dimethyl sulfide. *Microbiology* **156**(Pt 6):1900 – 1906. DOI: 10.1099/mic.0.038927-0, PMID: 20378650

**Kovach ME**, Elzer PH, Hill DS, Robertson GT, Farris MA, Roop 2nd RM, Peterson KM. 1995. Four new derivatives of the broad-host-range cloning vector pBBR1MCS, carrying different antibiotic-resistance cassettes. *Gene* **166**:175-176. DOI: 10.1016/0378-1119(95)00584-1, PMID: 8529885

**Kumar S**, Stecher G, Tamura K. 2016. MEGA7: Molecular evolutionary genetics analysis version 7.0 for bigger datasets. *Molecular Biology and Evolution* **33**:1870-1874. DOI: 10.1093/molbev/msw054, PMID: 27004904

**Lane DJ**, Pace B, Olsen GJ, Stahl DA, Sogin ML, Pace NR. 1985. Rapid determination of 16S ribosomal RNA sequences for phylogenetic analyses. *PNAS* **82**:6955-6959. DOI: 10.1073/pnas.82.20.6955, PMID: 2413450

**Lei L**, Cherukuri KP, Alcolombri U, Meltzer D, Tawfik DS. 2018. The dimethylsulfoniopropionate (DMSP) lyase and lyase-like cupin family consists of *bona fide* DMSP lyases as well as other enzymes with unknown function. *Biochemistry* **57**:3364-3377. DOI: 10.1021/acs.biochem.8b00097, PMID: 29561599

**Li CY**, Wei TD, Zhang SH, Chen XL, Gao X, Wang P, Xie BB, Su HN, Qin QL, Zhang XY, Yu J, Zhang HH, Zhou BC, Yang GP, Zhang YZ. 2014. Molecular insight into bacterial cleavage of oceanic dimethylsulfoniopropionate into demethyl sulfide. *PNAS* **111**: 1026 – 1031. DOI: 10.1073/pnas.1312354111, PMID: 24395783

**Li CY**, Zhang D, Chen XL, Wang P, Shi WL, Li PY, Zhang XY, Qin QL, Todd JD, Zhang YZ. 2017. Mechanistic insights into dimethylsulfoniopropionate lyase DddY, a new member of the cupin superfamily. *Journal of Molecular Biology* **429**:3850-3862. DOI: 10.1016/j.jmb.2017.10.022, PMID: 29106934

**Liu J**, Liu J, Zhang SH, Liang J, Lin H, Song D, Yang GP, Todd JD, Zhang XH. 2018. Novel insights

into bacterial dimethylsulfoniopropionate catabolism in the East China Sea. *Frontiers in Microbiology* **9**:3206. DOI: 10.3389/fmicb.2018.03206, PMID: 30622530

**Mai X**, Adams MWW. 1996. Purification and characterization of two reversible and ADP-dependent acetyl coenzyme A synthetases from the hyperthermophilic archaeon *Pyrococcus furiosus*. *Journal of Bacteriology* **178**:5897-5903. DOI: 10.1128/jb.178.20.5897-5903.1996, PMID: 8830684

**Minor W**, Cymborowski M, Otwinowski Z, Chruszcz M. 2006. HKL-3000: the integration of data reduction and structure solution - from diffraction images to an initial model in minutes. *Acta Crystallographica Section D-Structural Biology* **62**:859-866. DOI: 10.1107/S0907444906019949, PMID: 16855301

**Musfeldt M**, Schonheit P. 2002. Novel type of ADP-forming acetyl coenzyme A synthetase in hyperthermophilic archaea: heterologous expression and characterization of isoenzymes from the sulfate reducer *Archaeoglobus fulgidus* and the methanogen *Methanococcus jannaschii*. *Journal of Bacteriology* **184**:636-644. doi: 10.1128/jb.184.3.636-644.2002, PMID: 11790732

**Nevitt GA**. 2011. The neuroecology of dimethyl sulfide: a global-climate regulator turned marine infochemical. *Integrative and Comparative Biology* **51**:819-825. DOI: 10.1093/icb/icr093, PMID: 21880692

**Otte ML**, Wilson G, Morris JT, Moran BM. 2004. Dimethylsulphoniopropionate (DMSP) and related compounds in higher plants. *Journal of Experimental Botany* **55**:1919-1925. DOI: 10.1093/jxb/erh178, PMID: 15181109

**Patel SS**, Walt DR. 1987. Substrate specificity of acetyl coenzyme A synthetase. *Journal of Biological Chemistry* **262**:7132-7134. DOI: 10.0000/PMID2884217, PMID: 2884217

**Peng M**, Chen XL, Zhang D, Wang XJ, Wang N, Wang P, Todd JD, Zhang YZ, Li CY. 2019. Structure-function analysis indicates that an active-site water molecule participates in dimethylsulfoniopropionate cleavage by DddK. *Applied and Environmental Microbiology* **85**:e03127-18. DOI: 10.1128/AEM.03127-18, PMID: 30770407

**Raina JB**, Tapiolas DM, Forêt S, Lutz A, Abrego D, Ceh J, Seneca FO, Clode PL, Bourne DG, Willis BL, Motti CA. 2013. DMSP biosynthesis by an animal and its role in coral thermal stress response. *Nature* **502**:677-680. DOI: 10.1038/nature12677, PMID: 24153189

**Reisch CR**, Crabb WM, Gifford SM, Teng Q, Stoudemayer MJ, Moran MA, Whitman WB. 2013. Metabolism of dimethylsulphoniopropionate by *Ruegeria pomeroyi* DSS-3. *Molecular Microbiology* **89**:774-791. DOI: 10.1111/mmi.12314, PMID: 23815737

**Reisch CR**, Moran MA, Whitman WB. 2008. Dimethylsulfoniopropionate-dependent demethylase (DmdA) from *Pelagibacter ubique* and *Silicibacter pomeroyi*. *Journal of Bacteriology* **190**:8018-8024. DOI: 10.1128/JB.00770-08, PMID: 18849431

**Reisch CR**, Moran MA, Whitman WB. 2011a. Bacterial catabolism of dimethylsulfoniopropionate (DMSP). *Frontiers in Microbiology* **2**:172. DOI: 10.3389/fmicb.2011.00172, PMID: 21886640

**Reisch CR**, Stoudemayer MJ, Varaljay VA, Amster IJ, Moran MA, Whitman WB. 2011b. Novel pathway for assimilation of dimethylsulphoniopropionate widespread in marine bacteria. *Nature* **473**:208-211. DOI: 10.1038/nature10078, PMID: 21562561

**Sánchez LB**, Galperin MY, Müller M. 2000. Acetyl-CoA synthetase from the amitochondriate

eukaryote *Giardia lamblia* belongs to the newly recognized superfamily of acyl-CoA synthetases (Nucleoside diphosphate-forming). *Journal of Biological Chemistry* **275**:5794-5803. DOI: 10.1074/jbc.275.8.5794, PMID: 10681568

**Schlitzer R.** 2002. Interactive analysis and visualization of geoscience data with Ocean Data View. *Computers & Geosciences* **28**:1211-1218. DOI:10.1016/S0098-3004(02)00040-7

**Seymour JR,** Simó R, Ahmed T, Stocker R. 2010. Chemoattraction to dimethylsulfoniopropionate throughout the marine microbial food web. *Science* **329**:342-345. DOI: 10.1126/science.1188418, PMID: 20647471

**Shao X,** Cao HY, Zhao F, Peng M, Wang P, Li CY, Shi WL, Wei TD, Yuan ZL, Zhang XH, Chen XL, Todd JD, Zhang YZ. 2019. Mechanistic insight into 3-methylmercaptopropionate metabolism and kinetical regulation of demethylation pathway in marine dimethylsulfoniopropionate-catabolizing bacteria. *Molecular Microbiology* **111**:1057-1073. DOI: 10.1111/mmi.14211, PMID: 30677184

**Stefels JP.** 2000. Physiological aspects of the production and conversion of DMSP in marine algae and higher plants. *Journal of Sea Research* **43**:183-197. DOI: 10.1016/S1385-1101(00)00030-7

**Sunda W,** Kieber DJ, Kiene RP, Huntsman S. 2002. An antioxidant function for DMSP and DMS in marine algae. *Nature* **418**:317-320. DOI: 10.1038/nature00851, PMID: 12124622

**Sun L,** Curson ARJ, Todd JD, Johnston AWB. 2012. Diversity of DMSP transport in marine bacteria, revealed by genetic analyses. *Biogeochemistry* **110**:121-130. DOI: <https://doi.org/10.1007/s10533-011-9666-z>

**Thume K,** Gebser B, Chen L, Meyer N, Kieber DJ, Pohnert G. 2018. The metabolite dimethylsulfoxonium propionate extends the marine organosulfur cycle. *Nature* **563**:412-415. DOI: 10.1038/s41586-018-0675-0, PMID: 30429546

**Todd JD,** Curson ARJ, Dupont CL, Nicholson P, Johnston AWB. 2009. The *dddP* gene, encoding a novel enzyme that converts dimethylsulfoniopropionate into dimethyl sulfide, is widespread in ocean metagenomes and marine bacteria and also occurs in some Ascomycete fungi. *Environmental Microbiology* **11**:1376-1385. DOI: 10.1111/j.1462-2920.2009.01864.x, PMID: 19220400

**Todd JD,** Curson ARJ, Kirkwood M, Sullivan MJ, Green RT, Johnston AWB. 2011. DddQ, a novel, cupin-containing, dimethylsulfoniopropionate lyase in marine roseobacters and in uncultured marine bacteria. *Environmental Microbiology* **13**:427-438. DOI: 10.1111/j.1462-2920.2010.02348.x, PMID: 20880330

**Todd JD,** Curson ARJ, Nikolaidou-Katsaraidou N, Brearley CA, Watmough NJ, Chan Y, Page PCB, Sun L, Johnston AWB. 2010. Molecular dissection of bacterial acrylate catabolism-unexpected links with dimethylsulfoniopropionate catabolism and dimethyl sulfide production. *Environmental Microbiology* **12**:327-343. DOI: 10.1111/j.1462-2920.2009.02071.x, PMID: 19807777

**Todd JD,** Curson ARJ, Sullivan MJ, Kirkwood M, Johnston AWB. 2012. The *Ruegeria pomeroyi acul* gene has a role in DMSP catabolism and resembles *yhdH* of *E. coli* and other bacteria in conferring resistance to acrylate. *PLOS ONE* **7**:e35947. DOI: 10.1371/journal.pone.0035947, PMID: 22563425

**Todd JD,** Rogers R, Li YG, Wexler M, Bond PL, Sun L, Curson ARJ, Malin G, Steinke M, Johnston AWB. 2007. Structural and regulatory genes required to make the gas dimethyl sulfide in bacteria. *Science* **315**:666-669. DOI: 10.1126/science.1135370, PMID: 17272727

- Vallina SM**, Simó R. 2007. Strong relationship between DMS and the solar radiation dose over the global surface ocean. *Science* **315**:506-508. DOI: 10.1126/science.1133680, PMID: 17255509
- van der Maarel M**, Van Bergeijk S, Van Werkhoven AF, Laverman AM, Meijer WG, Stam WT, Hansen TA. 1996. Cleavage of dimethylsulfoniopropionate and reduction of acrylate by *Desulfovibrio acrylicus* sp. nov. *Archives of Microbiology* **166**:109-115. DOI: 10.1007/s002030050363
- Verschueren KHG**, Blanchet C, Felix J, Dansercoer A, Vos DD, Bloch Y, Beeumen JV, Svergun D, Gutsche I, Savvides SN, Verstraete K. 2019. Structure of ATP citrate lyase and the origin of citrate synthase in the Krebs cycle. *Nature* **568**:571-575. DOI: 10.1038/s41586-019-1095-5, PMID: 30944476
- Wang P**, Cao HY, Chen XL, Li CY, Li PY, Zhang XY, Qin QL, Todd JD, Zhang YZ. 2017. Mechanistic insight into acrylate metabolism and detoxification in marine dimethylsulfoniopropionate-catabolizing bacteria. *Molecular Microbiology* **105**:674-688. DOI: 10.1111/mmi.13727, PMID: 28598523
- Wang P**, Chen XL, Li CY, Gao X, Zhu DY, Xie BB, Qin QL, Zhang XY, Su HN, Zhou BC, Xun LY, Zhang YZ. 2015. Structural and molecular basis for the novel catalytic mechanism and evolution of DddP, an abundant peptidase-like bacterial dimethylsulfoniopropionate lyase: a new enzyme from an old fold. *Molecular Microbiology* **98**:289 – 301. DOI: 10.1111/mmi.13119, PMID: 26154071
- Wang PX**, Yu ZC, Li BY, Cai XS, Zeng ZS, Chen XL, Wang XX. 2015. Development of an efficient conjugation-based genetic manipulation system for *Pseudoalteromonas*. *Microbial Cell Factories* **14**:11. DOI: 10.1186/s12934-015-0194-8, PMID: 25612661
- Weiß RHJ**, Faust A, Schmidt M, Schönheit P, Scheidig AJ. 2016. Structure of NDP-forming Acetyl-CoA synthetase ACD1 reveals a large rearrangement for phosphoryl transfer. *PNAS* **113**:E519-528. DOI: 10.1073/pnas.1518614113, PMID: 26787904
- Winn MD**, Ballard CC, Cowtan KD, Dodson EJ, Emsley P, Evans PR, Keegan RM, Krissinel EB, Leslie AGW, McCoy A, McNicholas SJ, Murshudov GN, Pannu NS, Potterton EA, Powell HR, Read RJ, Vagin A, Wilson KS. 2011. Overview of the CCP4 suite and current developments. *Acta Crystallographica Section D-Structural Biology* **67**:235-242. DOI: 10.1107/S0907444910045749, PMID: 21460441
- Wolfe GV**, Steinke M, Kirst GO. 1997. Grazing-activated chemical defence in a unicellular marine alga. *Nature* **387**:894–897. DOI: 10.1038/43168
- Yoon SH**, Ha SM, Kwon S, Lim J, Kim Y, Seo H, Chun J. 2017. Introducing EzBioCloud: a taxonomically united database of 16S rRNA gene sequences and whole-genome assemblies. *International Journal of Systematic Evolutionary Microbiology* **67**:1613-1617. DOI: 10.1099/ijsem.0.001755, PMID: 28005526
- You D**, Wang MM, Ye BC. 2017. Acetyl-CoA synthetases of *Saccharopolyspora erythraea* are regulated by the nitrogen response regulator GlnR at both transcriptional and post-translational levels. *Molecular Microbiology* **103**:845-859. DOI: 10.1111/mmi.13595, PMID: 27987242
- Zhang XH**, Liu J, Liu JL, Yang GP, Xue CX, Curson ARJ, Todd TD. 2019. Biogenic production of DMSP and its degradation to DMS-their roles in the global sulfur cycle. *Science China Life Sciences* **62**:1296-1319. DOI: 10.1007/s11427-018-9524-y, PMID: 31231779
- Zheng YF**, Wang JY, Zhou S, Zhang YH, Liu J, Xue CX, Williams BT, Zhao XX, Zhao L, Zhu XY,

Sun C, Zhang HH, Xiao T, Yang GP, Todd TD, Zhang XH. 2020. Bacteria are important dimethylsulfoniopropionate producers in marine aphotic and high-pressure environments. *Nature Communications* **11**:4658. DOI: 10.1038/s41467-020-18434-4, PMID: 32938931

## Acknowledgments

We thank the staffs from BL18U1 & BL19U1 beamlines of National Facility for Protein Sciences Shanghai (NFPS) and Shanghai Synchrotron Radiation Facility, for assistance during data collection. We thank Caiyun Sun and Jingyao Qu from State Key laboratory of Microbial Technology of Shandong University for their help in HPLC and LC-MS. **Funding:** This work was supported by the National Key Research and Development Program of China (2018YFC1406700, 2016YFA0601303), the National Science Foundation of China (grants 91851205, 31630012, U1706207, 42076229, 31870052, 31800107), Major Scientific and Technological Innovation Project (MSTIP) of Shandong Province (2019JZZY010817), the Program of Shandong for Taishan Scholars (tspd20181203) and Natural Environment Research Council Standard grants (NE/N002385, NE/P012671 and NE/S001352).

## Competing interests

Authors declare no competing interests.

## Supplementary files

Supplementary file 1a. Information of the Antarctic samples used in this study.

880     Supplementary file 1b. Homology alignment of proteins in *Psychrobacter* sp. D2 with  
881     known DMSP lyases.

882     Supplementary file 1c. Kinetic parameters of DMSP lyases and DMSP demethylase  
883     DmdA.

884     Supplementary file 1d. Crystallographic data collection and refinement parameters of  
885     DddX.

886     Supplementary file 1e. Homology alignment of proteins in *Psychrobacter* sp. D2 with  
887     known enzymes involved in acrylate catabolism.

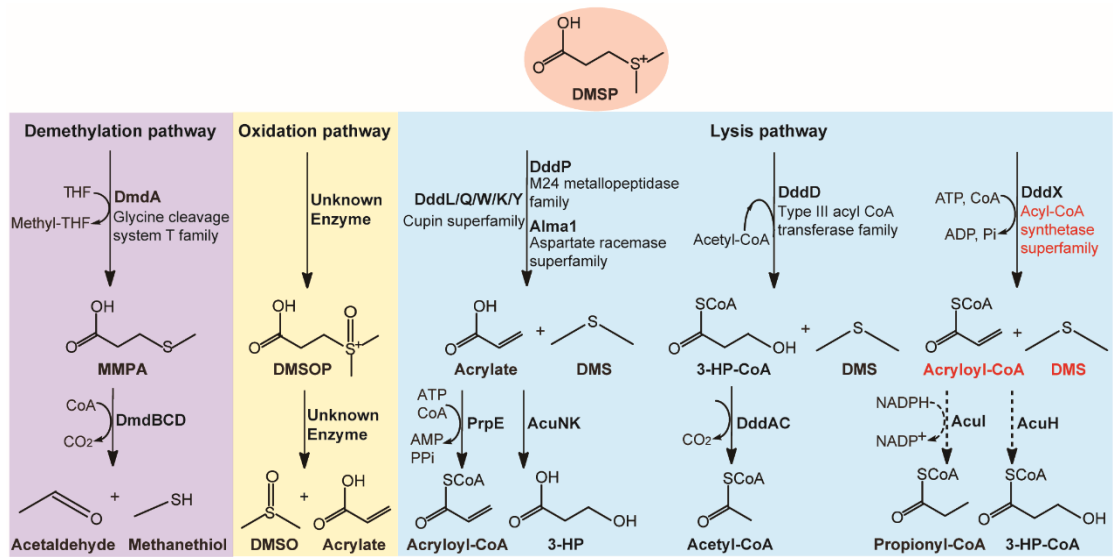
888     Supplementary file 1f. Strains and plasmids used in this study.

889     Supplementary file 1g. Composition of the basal medium (lacking the carbon source).

890     Supplementary file 1h. Primers used in this study.

891     Transparent reporting form.

892



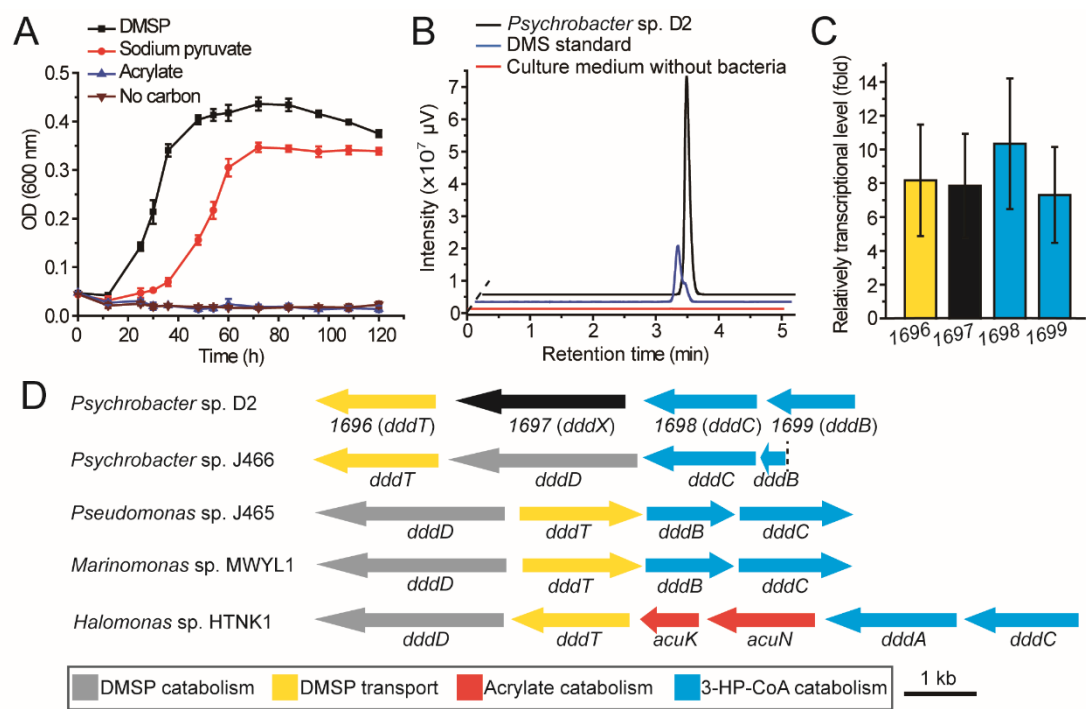
894

895 **Figure 1. Metabolic pathways for DMSP degradation.** Different pathways are shown in different  
896 colors. The demethylation of DMSP by DmdA produces MMPA (in purple). The oxidation of  
897 DMSP produces DMSOP (in yellow). In the lysis pathway (in blue), DMSP lyase DddP, DddL,  
898 DddQ, DddW, DddK, DddY or Alma1 converts DMSP to acrylate and DMS, DddD converts  
899 DMSP to 3-HP-CoA and DMS, using acetyl-CoA as a CoA donor, and the newly identified DddX  
900 in this study converts DMSP to acryloyl-CoA and DMS, with ATP and CoA as co-substrates.  
901 Dotted lines represent unconfirmed steps of the DddX DMSP lysis pathway that we propose in  
902 this study. The protein families of enzymes involved in the first step of each pathway are indicated.  
903 The protein family of DddX and the products of its catalysis are highlighted in red color.  
904 Abbreviations: THF, tetrahydrofolate; MMPA, methylmercaptopropionate; 3-HP,  
905 3-hydroxypropionate; DMSOP, dimethylsulfoxonium propionate; DMSO, dimethylsulfoxide.

906 **Figure 1-figure supplement 1.** Enzymatic activity analysis of the recombinant DddX using  
907 acetyl-CoA as a CoA donor. ATP and acetyl-CoA were analyzed by HPLC through its ultraviolet

absorbance under 260 nm. The result showed that DddX failed to catalyze the degradation of DMSP when acetyl-CoA was used as a CoA donor.

**Figure 1-figure supplement 2.** HPLC assay of the enzymatic activity of 0105 protein on acryloyl-CoA at 260 nm. The peak of acryloyl-CoA was indicated with black arrow and the peak of propionate-CoA was indicated with red arrow. The recombinant 0105 could catalyze the conversion of acryloyl-CoA to propionate-CoA ( $718.3 \pm 59.2$  pmol propionate-CoA min<sup>-1</sup> mg protein<sup>-1</sup>). The reaction system without 0105 protein was used as the control.



917

918 **Figure 2. The utilization of DMSP by *Psychrobacter* sp. D2 and the putative**  
919 **DMSP-catabolizing gene cluster in its genome. A,** The growth curve of *Psychrobacter* sp. D2  
920 on DMSP, sodium pyruvate or acrylate as sole carbon source (5 mM) at 15°C. The error bar  
921 represents standard deviation of triplicate experiments. **B,** GC detection of DMS production from  
922 DMSP by strain D2. The culture medium without bacteria was used as the control. The DMS  
923 standard was used as a positive control. *Psychrobacter* sp. D2 could catabolize DMSP and produce  
924 DMS ( $44.8 \pm 1.8$  nmol DMS  $\text{min}^{-1}$  mg protein $^{-1}$ ). **C,** RT-qPCR assay of the transcriptions of the  
925 genes 1696, 1697, 1698 and 1699 in *Psychrobacter* sp. D2 in response to DMSP in the marine  
926 broth 2216 medium. The bacterium cultured without DMSP in the same medium was used as the  
927 control. The *recA* gene was used as an internal reference. The error bar represents standard  
928 deviation of triplicate experiments. The locus tags of 1696, 1697, 1698 and 1699 are  
929 H0262\_08195, H0262\_08200, H0262\_08205 and H0262\_08210, respectively. **D,** Genetic  
930 organization of the putative DMSP-catabolizing gene cluster. Reported DMSP catabolic/transport

gene clusters from *Psychrobacter* sp. J466, *Pseudomonas* sp. J465, *Marinomonas* sp. MWYL1 and *Halomonas* sp. HTNK1 are shown (Todd et al., 2007; Todd et al., 2010; Curson et al., 2010; Curson et al., 2011b). The dashed vertical line indicates a breakpoint in *dddB* in the cosmid library of *Pseudomonas* sp. J466 (Curson et al., 2010).

**Figure 2-source data 1.** The growth curve of *Psychrobacter* sp. D2 on DMSP, sodium pyruvate or acrylate as sole carbon source.

**Figure 2-source data 2.** GC detection of DMS production from DMSP by strain D2.

**Figure 2-source data 3.** RT-qPCR assay of the transcriptions of the genes *1696*, *1697*, *1698* and *1699* in *Psychrobacter* sp. D2.

**Figure 2-figure supplement 1.** Locations of the sampling sites and the relative abundance of DMSP-catabolizing bacteria isolated from the samples. **A**, Locations of the sampling sites in the Antarctic. Stations were plotted using Ocean Data View (Schlitzer, 2002). **B**, The relative abundance of DMSP-catabolizing bacteria isolated from the Antarctic samples. The detailed information of the samples is shown in Supplementary file 1a.

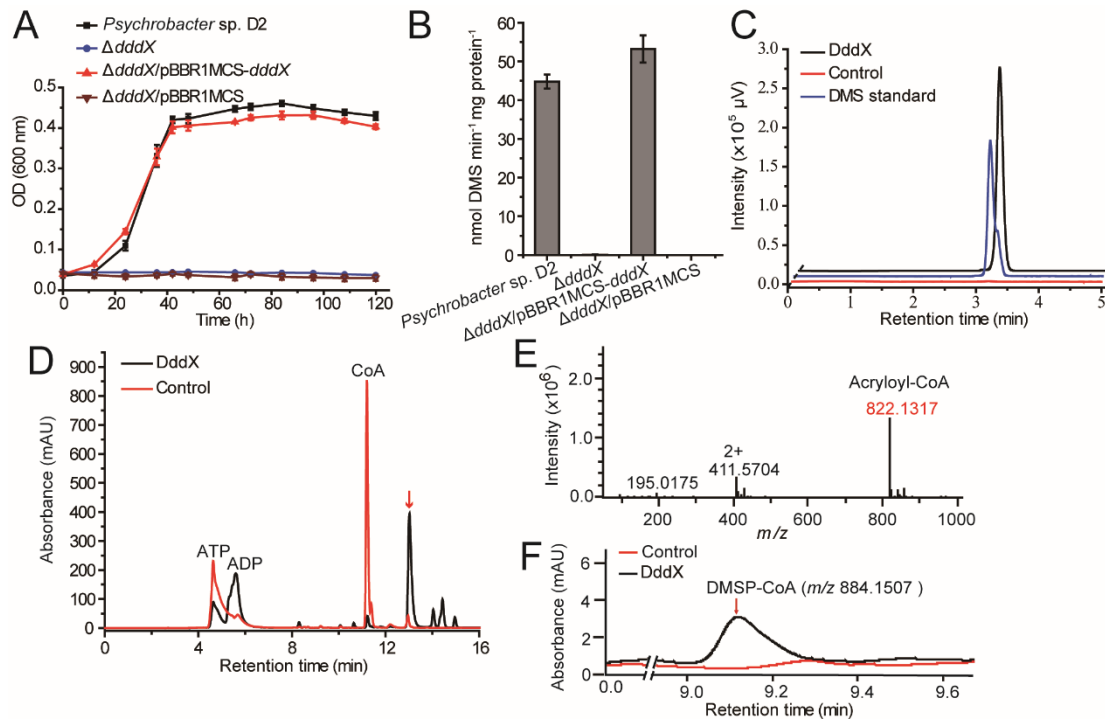
**Figure 2-figure supplement 1-source data 1.** The number of DMSP-catabolizing strains isolated from the Antarctic samples.

**Figure 2-figure supplement 2.** Transcriptomic analysis of the putative genes involved in DMSP metabolism in strain D2. The transcriptions of four genes in a cluster were significantly up-regulated during the growth of strain D2 on DMSP. The fold changes were calculated by comparing to the control (transcriptions of these genes during the strain growth on sodium pyruvate).

**Figure 2-figure supplement 2-source data 1.** Transcriptomic analysis of the putative genes involved in DMSP metabolism in strain D2.

**Figure 2-figure supplement 3.** Confirmation of the deletion of the *dddX* gene from

955 *Psychrobacter* sp. D2. Lane M, DNA marker; Lane 1, Wild-type *Psychrobacter* sp. D2; Lane 2,  
956 the  $\Delta dddX$  mutant. The  $\Delta dddX$  mutant generated a 1000 bp PCR product using the  
957 *dddX*-1000-F/*dddX*-1000-R primer set, while the product length was 3247 bp for the wild-type  
958 strain.  
959



961

**Figure 3. The function of *Psychrobacter* sp. D2 *dddX* in DMSP metabolism.** **A**, Growth curves of the wild-type strain D2, the  $\Delta dddX$  mutant, the complemented mutant ( $\Delta dddX/pBBR1MCS-dddX$ ), and the  $\Delta dddX$  mutant complemented with an empty vector ( $\Delta dddX/pBBR1MCS$ ). All strains were grown with DMSP (5 mM) as the sole carbon source. The error bar represents standard deviation of triplicate experiments. **B**, Detection of DMS production from DMSP degradation by the wild-type strain D2, the  $\Delta dddX$  mutant, the complemented mutant  $\Delta dddX/pBBR1MCS-dddX$ , and the mutant complemented with an empty vector  $\Delta dddX/pBBR1MCS$ . The error bar represents standard deviation of triplicate experiments. **C**, GC detection of DMS production from DMSP lysis catalyzed by the recombinant DddX. The reaction system without DddX was used as the control. DddX maintained a specific activity of ~8.0  $\mu\text{mol min}^{-1} \text{mg protein}^{-1}$  at 20°C, pH 8.0. **D**, HPLC analysis of the enzymatic activity of the recombinant DddX on DMSP at 260 nm. The peak of the unknown product is indicated with a red arrow. The

reaction system without DddX was used as the control. **E**, LC-MS analysis of the unknown product. **F**, HPLC analysis of the intermediate of DddX catalysis at 260 nm. The HPLC system was coupled to a mass spectrometer for  $m/z$  determination. The reaction system without DddX was used as the control.

**Figure 3-source data 1.** Growth curves of the wild-type strain D2, the  $\Delta dddX$  mutant, the complemented mutant ( $\Delta dddX/pBBR1MCS-dddX$ ), and the  $\Delta dddX$  mutant complemented with an empty vector ( $\Delta dddX/pBBR1MCS$ ).

**Figure 3-source data 2.** Detection of DMS production from DMSP degradation by the wild-type strain D2, the  $\Delta dddX$  mutant, the complemented mutant  $\Delta dddX/pBBR1MCS-dddX$ , and the mutant complemented with an empty vector  $\Delta dddX/pBBR1MCS$ .

**Figure 3-source data 3.** GC detection of DMS production from DMSP lysis catalyzed by the recombinant DddX.

**Figure 3-source data 4.** HPLC analysis of the enzymatic activity of the recombinant DddX on DMSP.

**Figure 3-figure supplement 1.** SDS-PAGE analysis of the recombinant DddX. The predicted molecular mass of the recombinant DddX is 81.62 kDa using the compute MW tool (*Gasteiger et al., 2005*).

**Figure 3-figure supplement 2.** Two alternative mechanisms for DMSP degradation catalyzed by DddX. **A**, DMSP is primarily cleaved to DMS and acrylate. Subsequently, CoA is ligated to acrylate producing acryloyl-CoA. **B**, CoA is primarily ligated to DMSP to produce DMSP-CoA, which is then cleaved to DMS and acryloyl-CoA.

**Figure 3-figure supplement 3.** Characterization of recombinant DddX. The error bar represents

standard deviation of triplicate experiments. A, Effect of temperature on DddX enzyme activity. B, Effect of pH on DddX enzyme activity. C, Kinetic parameters of DddX for ATP. D, Kinetic parameters of DddX for CoA. E, Kinetic parameters of DddX for DMSP.

**Figure 3-figure supplement 3-source data 1.** Characterization of recombinant DddX.

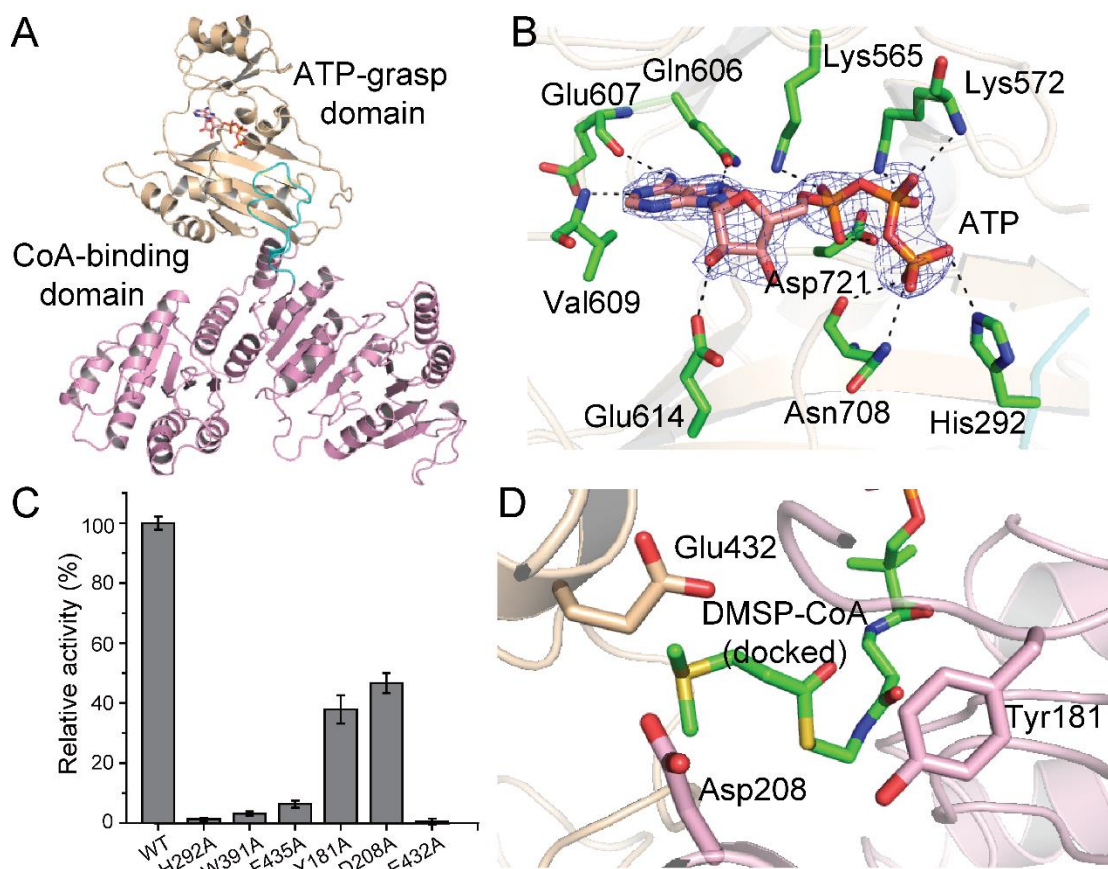
**Figure 3-figure supplement 4.** HPLC assay of the enzymatic activity of DddX towards DMSP, sodium acetate and sodium propionate at 260 nm. The peaks of ATP were indicated with black arrows, the peaks of CoA were indicated with red arrows, and the peak of acryloyl-CoA was indicated with the blue arrow. The reaction system without DddX was used as the control.

**Figure 3-figure supplement 5.** The effects of potential inhibitors on the enzymatic activity of DddX. SA, sodium acetate; SP, sodium propionate. The activity of DddX with no inhibitor was used as a reference (100%).

**Figure 3-figure supplement 5-source data 1.** The effects of potential inhibitors on the enzymatic activity of DddX.

**Figure 3-figure supplement 6.** The growth curves of *Psychrobacter* sp. D2 and the  $\Delta dddX$  mutant on sodium acetate (**A**) or sodium propionate (**B**) as the sole carbon source (5 mM) at 25°C. The error bar represents standard deviation of triplicate experiments.

**Figure 3-figure supplement 6-source data 1.** The growth curves of *Psychrobacter* sp. D2 and the  $\Delta dddX$  mutant on sodium acetate or sodium propionate as the sole carbon source.



1016

1017 **Figure 4. Structural and mutational analyses of DddX.** **A**, The overall structure of the DddX

1018 monomer. The DddX molecule contains a CoA-binding domain (colored in pink) and an

1019 ATP-grasp domain (colored in wheat). The loop region from the CoA-binding domain inserting

1020 into the ATP-grasp domain is colored in cyan. The ATP molecule is shown as sticks. **B**, Residues

1021 of DddX involved in binding ATP. The  $2F_o - F_c$  densities for ATP are contoured in blue at  $2.0\sigma$ .

1022 Residues of DddX involved in binding ATP are colored in green. **C**, Enzymatic activities of DddX

1023 and its mutants. The activity of WT DddX was taken as 100%. **D**, Structural analysis of the

1024 possible catalytic residues for the cleavage of DMSP-CoA. The docked DMSP-CoA molecule and

1025 the probable catalytic residues of DddX are shown as sticks.

1026 **Figure 4-source data 1.** Enzymatic activities of DddX and its mutants.

**Figure 4-figure supplement 1.** Structural and gel filtration analysis of DddX state of aggregation.

**A,** The overall structure of DddX tetramer. Different monomers are displayed in different colors.

**B,** Gel filtration analysis of DddX. Inset, semilog plot of the molecular mass of all standards used

versus their  $K_{av}$  values (black circles). The red spot indicates the position of the  $K_{av}$  value of DddX

interpolated in the regression line. DddX monomer has a molecular mass of 81.62 kDa.

**Figure 4-figure supplement 1-source data 1.** Gel filtration analysis of DddX.

**Figure 4-figure supplement 2.** The overall structure of ACD1. The  $\alpha$ -subunit and the  $\beta$ -subunit of

ACD1 (PDB code: 4xym) are colored in pink and wheat, respectively.

**Figure 4-figure supplement 3.** Sequence alignment of DddX homologs, acetyl-CoA synthetases

(ACS) and ATP-citrate lyases (ACLY). The conserved histidine residue is marked with a red star.

The swinging loop of DddX (Gly280-Tyr300) is indicated, which corresponds to the swinging

loop reported in acetyl-CoA synthetase ACD1 (Gly242-Val262) (*Weiß et al., 2016*).

**Figure 4-figure supplement 4.** CD spectra of WT DddX and its mutants.

**Figure 4-figure supplement 4-source data 1.** CD spectra of WT DddX and its mutants.

**Figure 4-figure supplement 5.** Structural analysis of DddX docked with DMSP and CoA, and

DMSP-CoA. **A.** The structure of DddX docked with DMSP and CoA. DMSP and CoA molecules

are shown as sticks. The surfaces of two DddX monomers are colored in wheat and pink,

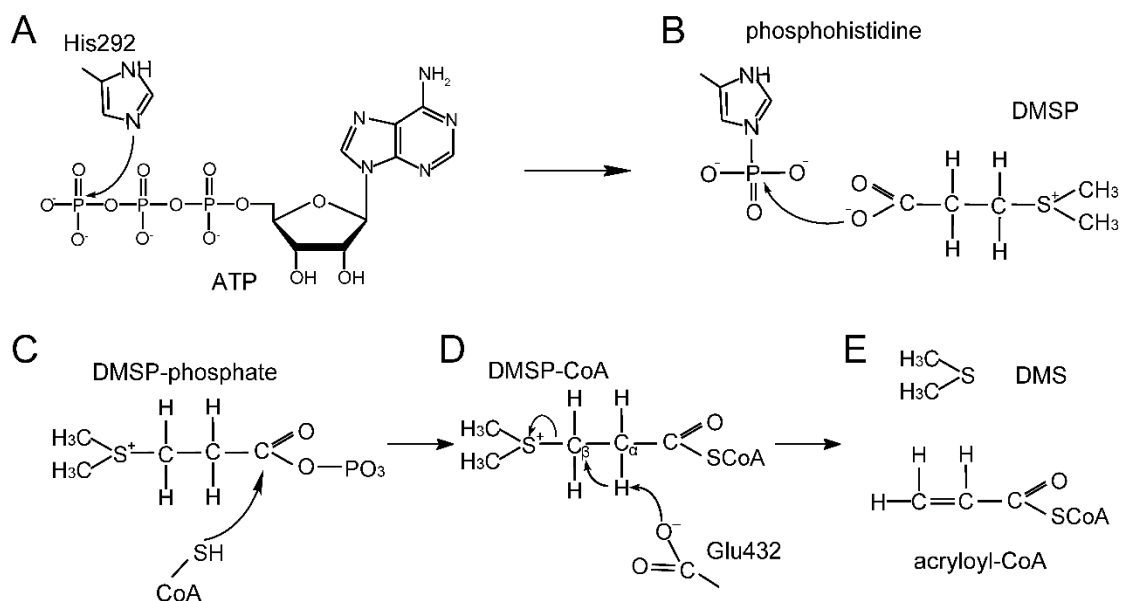
respectively. **B.** The structure of DddX docked with DMSP-CoA. DMSP-CoA is shown as sticks.

The surfaces of two DddX monomers are colored in wheat and pink, respectively. **C.** Structural

analysis of residues which form cation- $\pi$  interactions with the sulfonium group of DMSP-CoA.

DMSP-CoA and residues Trp391 and Phe435 are shown as sticks.

1049



1050

1051 **Figure 5. A proposed mechanism for DMSP cleavage to generate DMS and acryloyl-CoA**

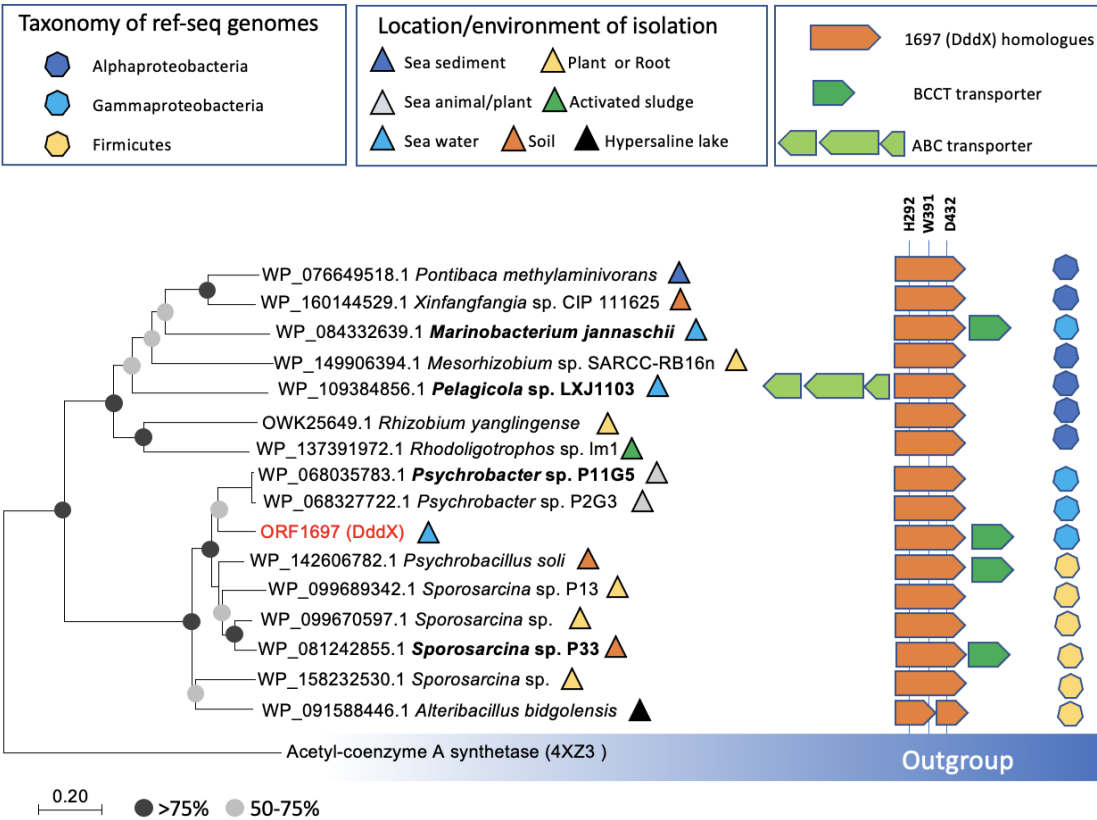
1052 **catalyzed by DddX. A,** The residue His292 attacks the  $\gamma$ -phosphate of ATP. **B,** The phosphoryl

1053 group is transferred from phosphohistidine to the DMSP molecule. **C,** DMSP-phosphate is

1054 attacked by CoA. **D,** The residue Glu432 acts as a general base to attack DMSP-CoA. **E,** DMS

1055 and acryloyl-CoA are generated.

1056

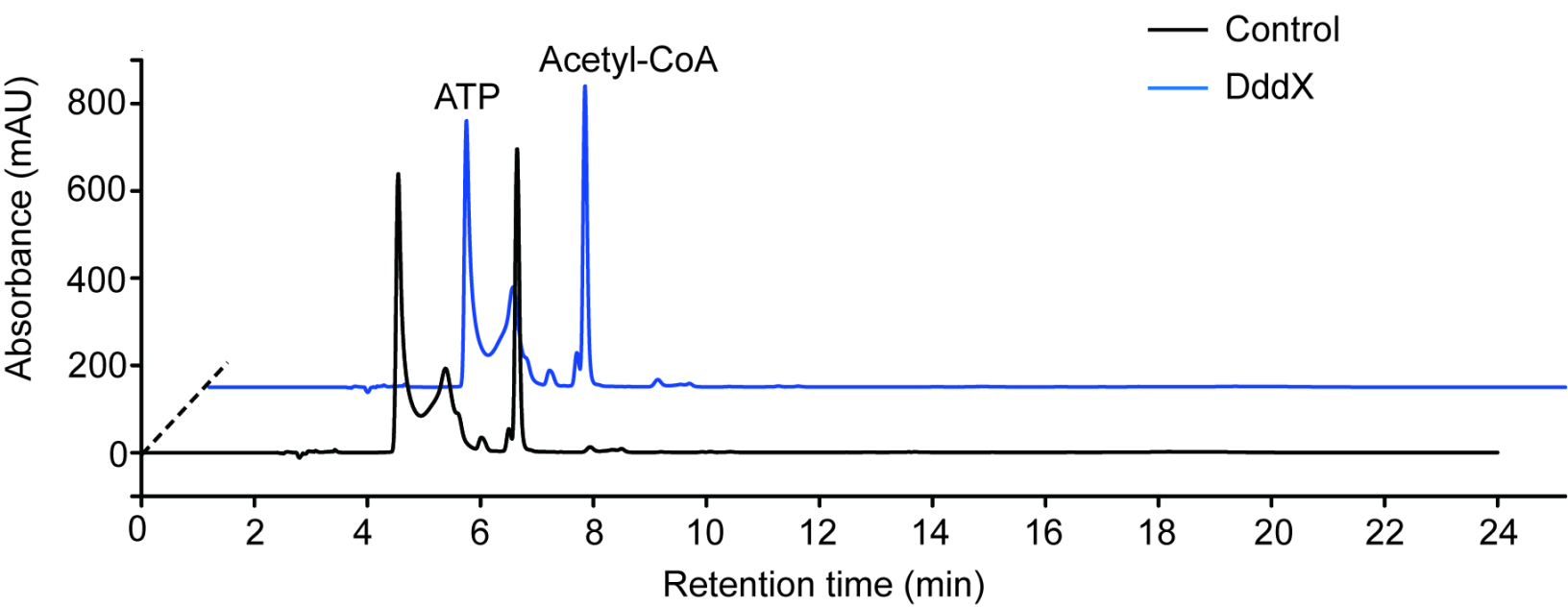


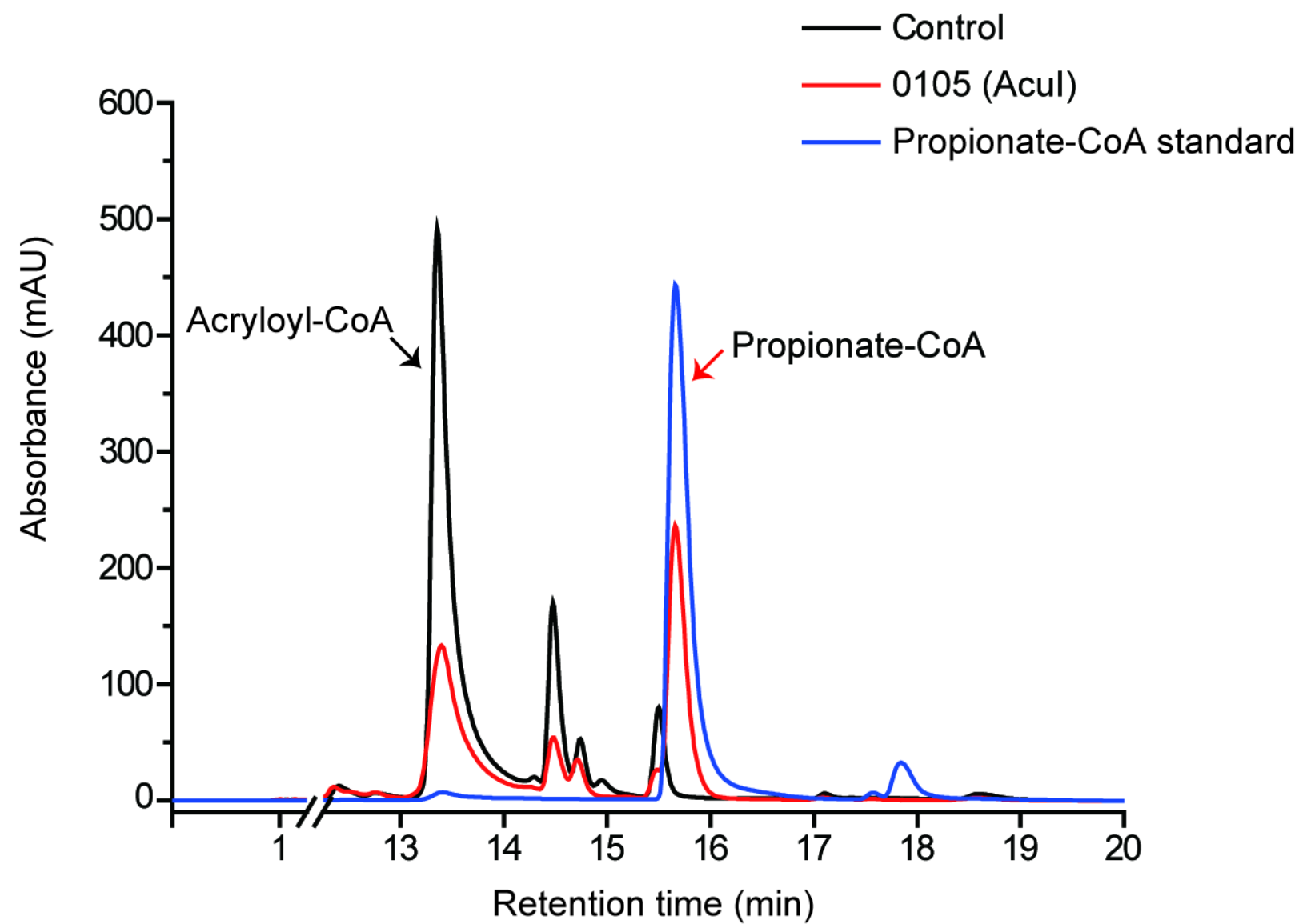
1058

1059 **Figure 6. Distribution of DddX in bacterial genomes.** The phylogenetic tree was constructed  
1060 using neighbor-joining method in MEGA7. The acetyl-coenzyme A synthetase (ACS) (*Weiße et*  
1061 *al., 2016*) was used as the outgroup. Sequence alignment was inspected for the presence of the key  
1062 histidine residue (His292) involved in histidine phosphorylation that is known to be important for  
1063 enzyme activity. A conserved Tyr391 is also found which is involved in cation- $\pi$  interaction with  
1064 DMSP. The BCCT-type or ABC-type transporters for betaine-carnitine-choline-DMSP were found  
1065 in the neighborhood of DddX in several genomes. Those DddX homologs that are functionally  
1066 characterized (*Figure 6-figure supplement 1*) are highlighted in bold.

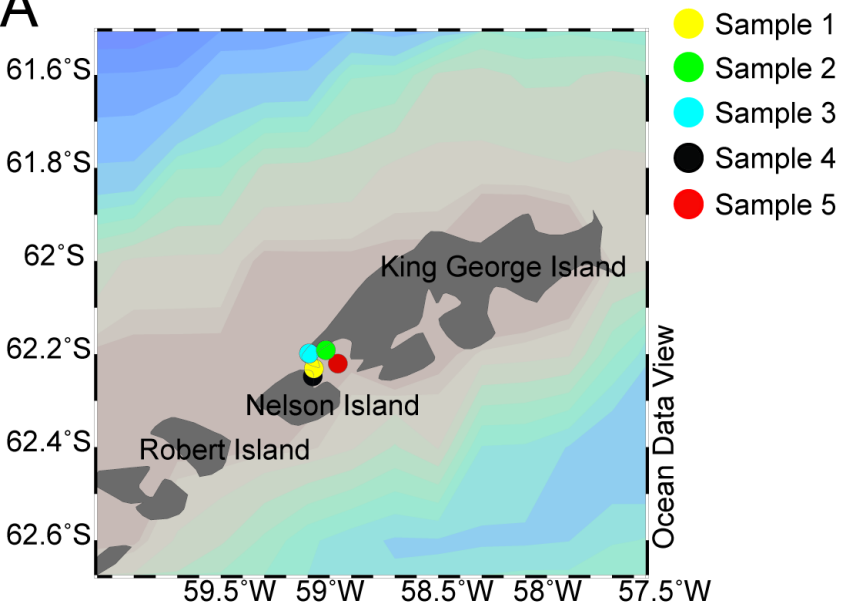
1067 **Figure 6-figure supplement 1.** HPLC assay of the enzymatic activity of DddX homologs on  
1068 DMSP at 260 nm. The peaks of acryloyl-CoA were indicated with red arrows and the peaks of

1069 CoA were indicated with black arrows. The reaction system without DddX was used as the  
1070 control.

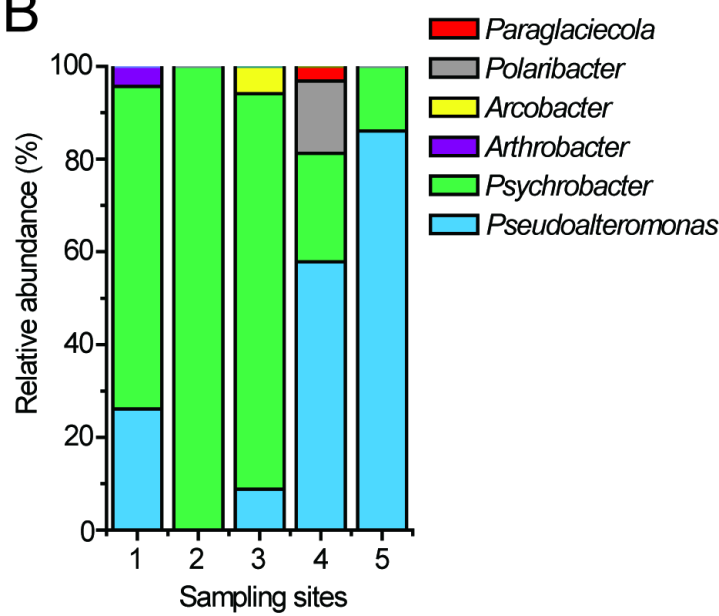


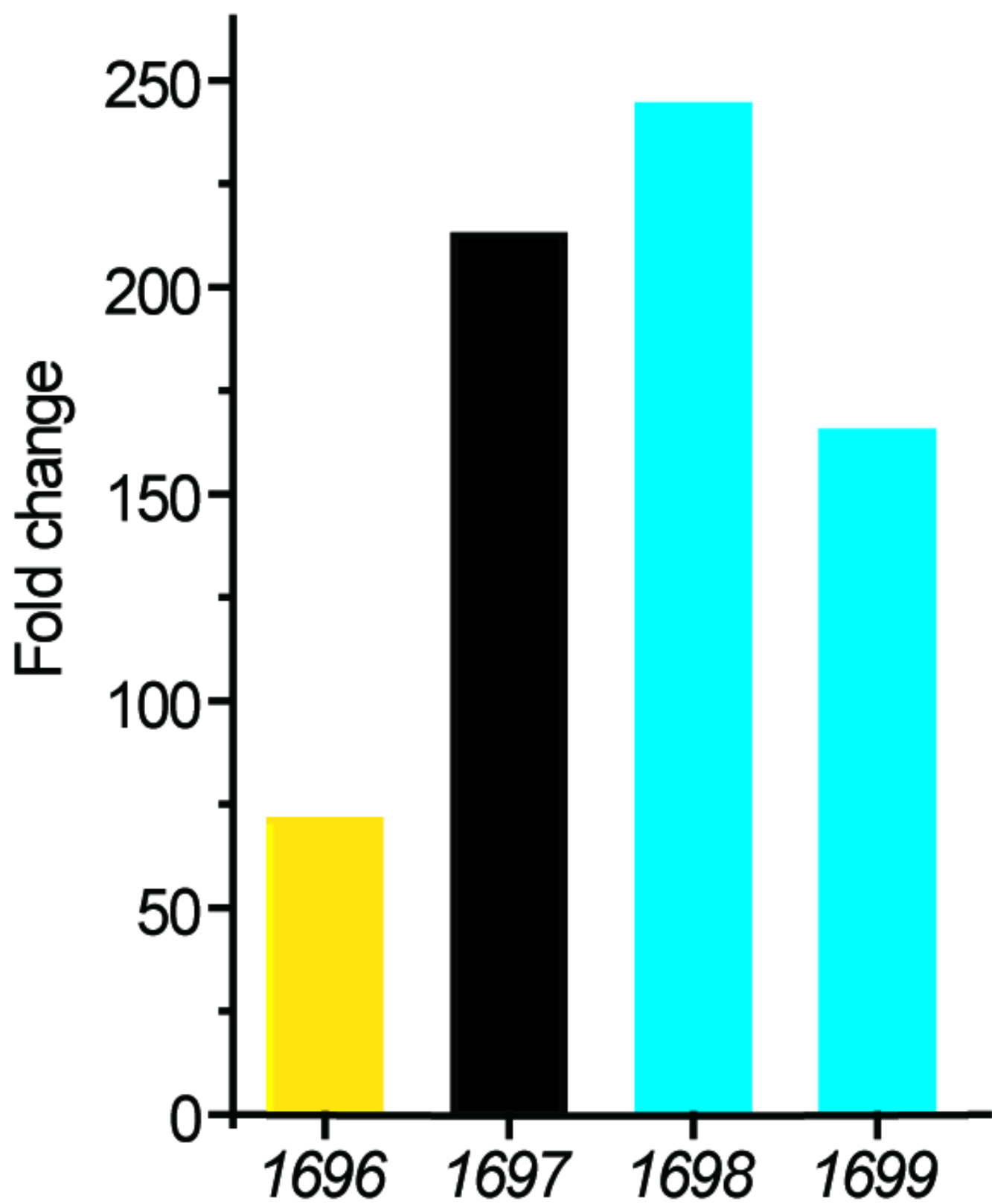


A



B





M

1

2

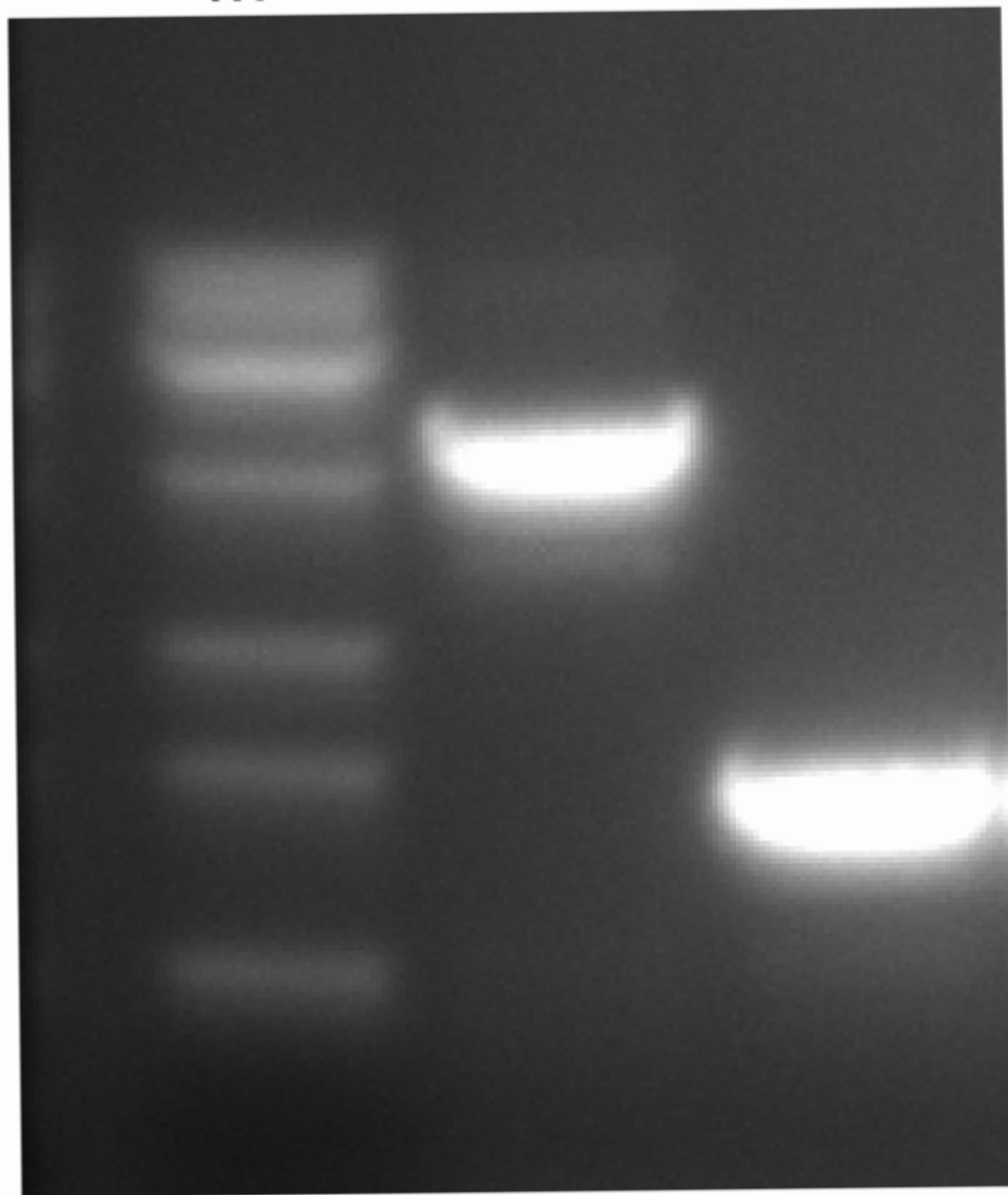
5000 bp

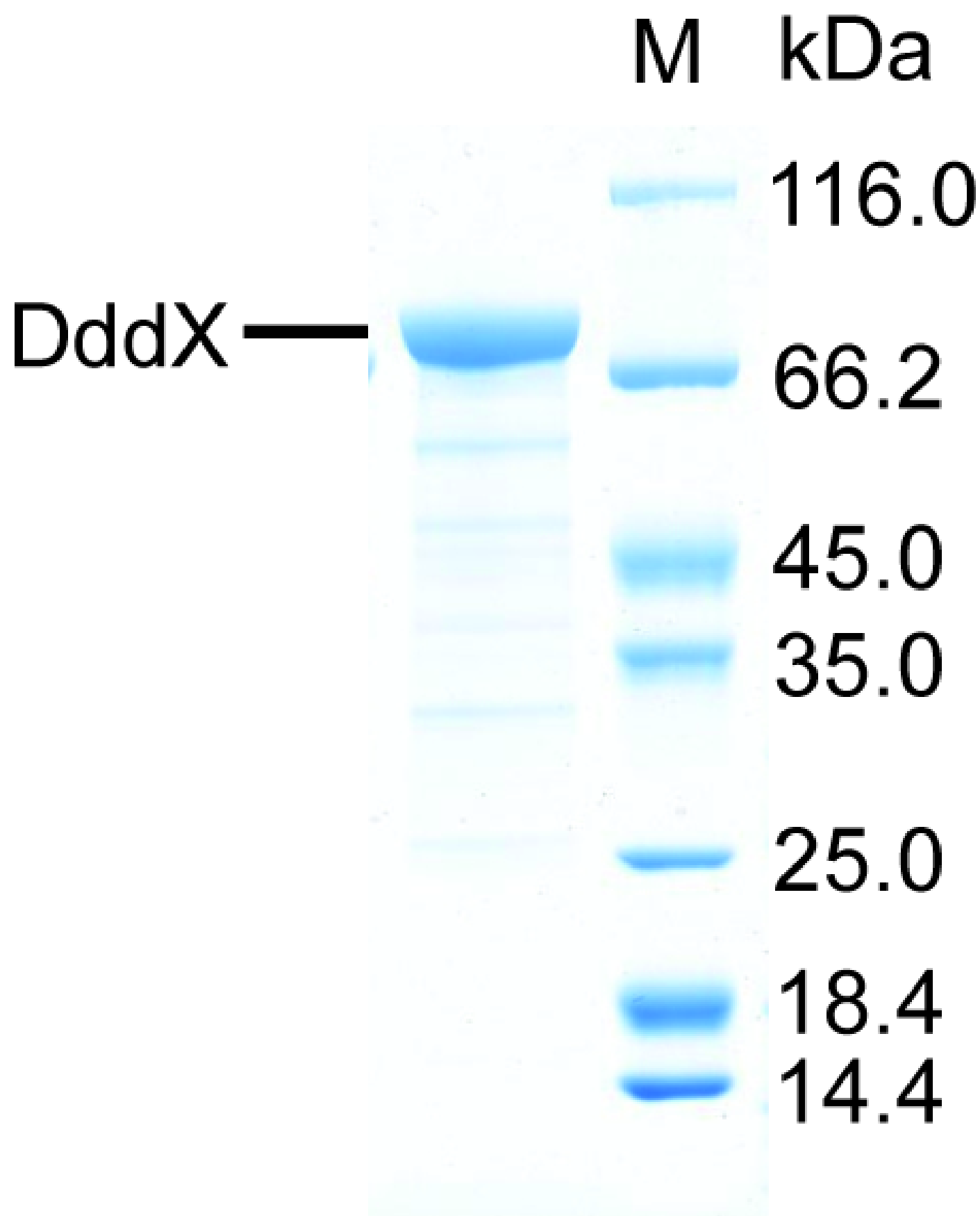
3000 bp

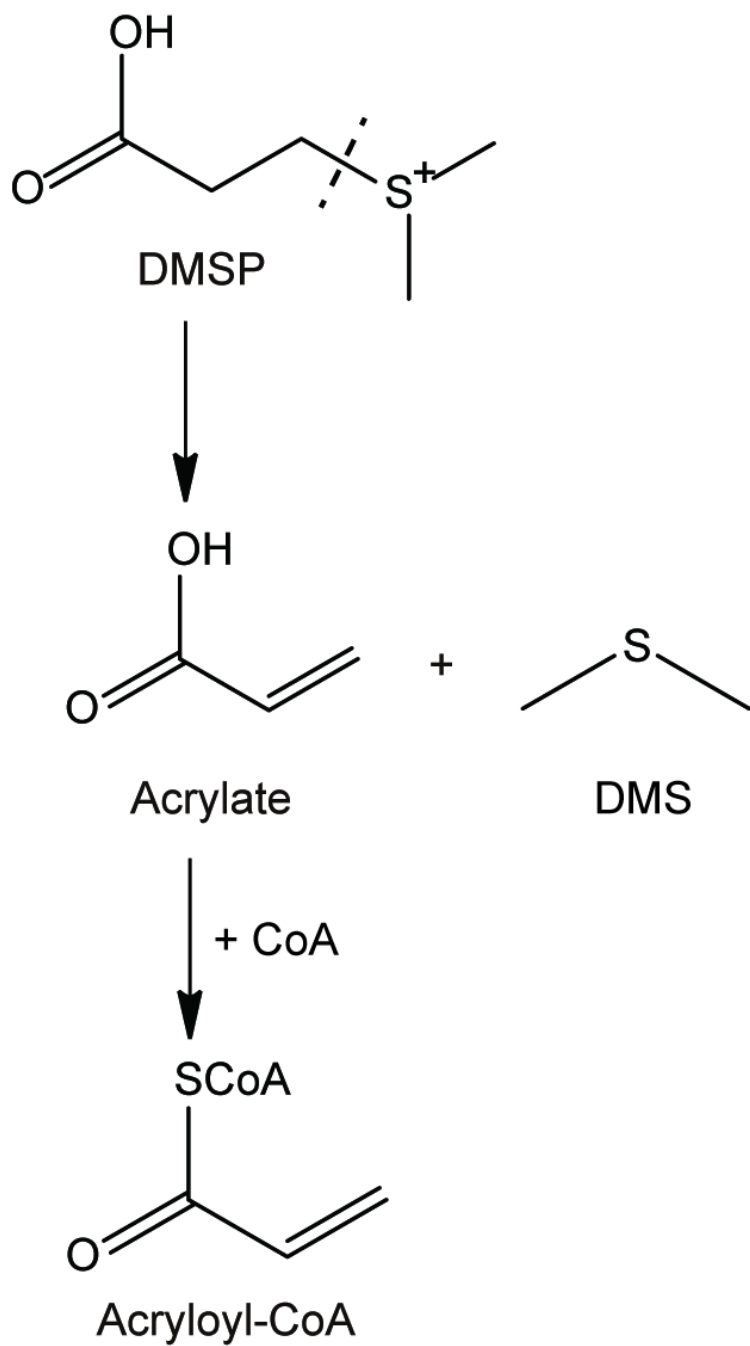
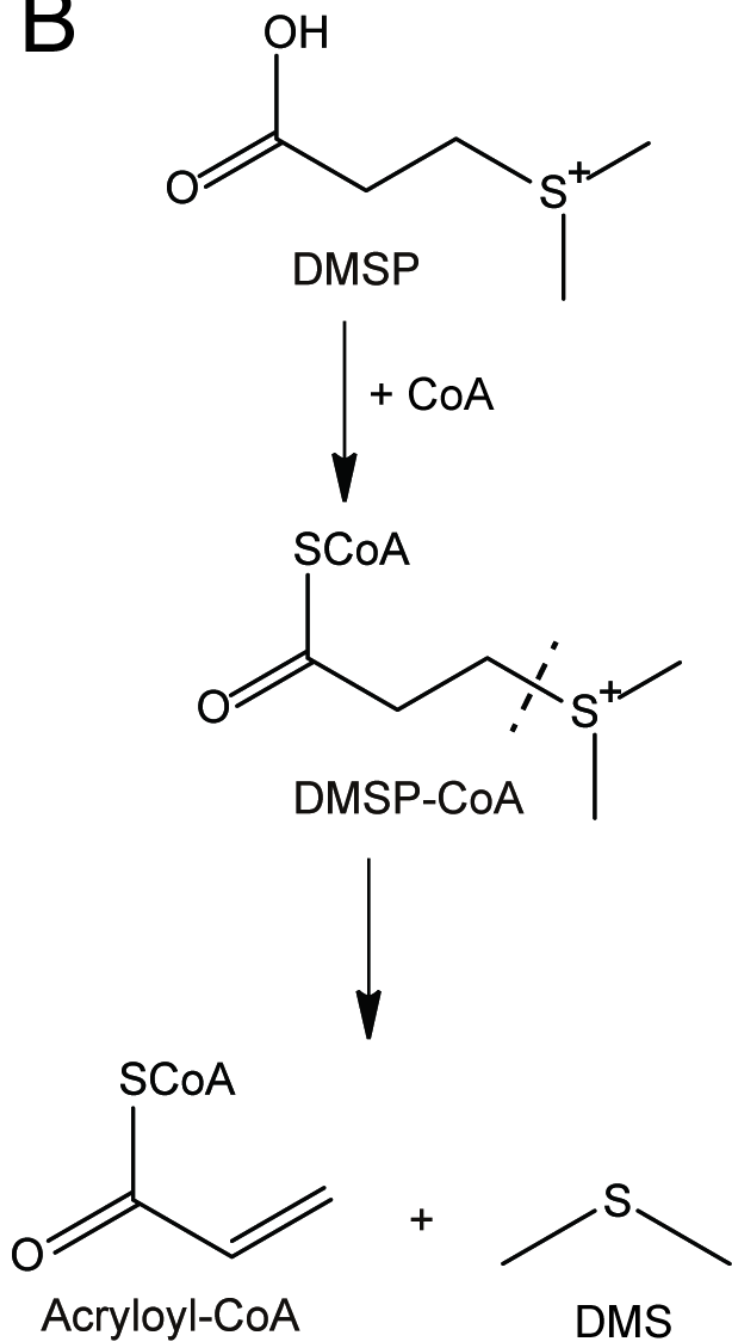
1500 bp

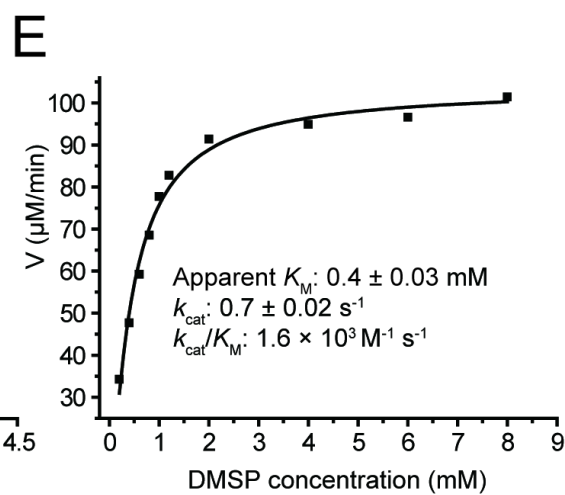
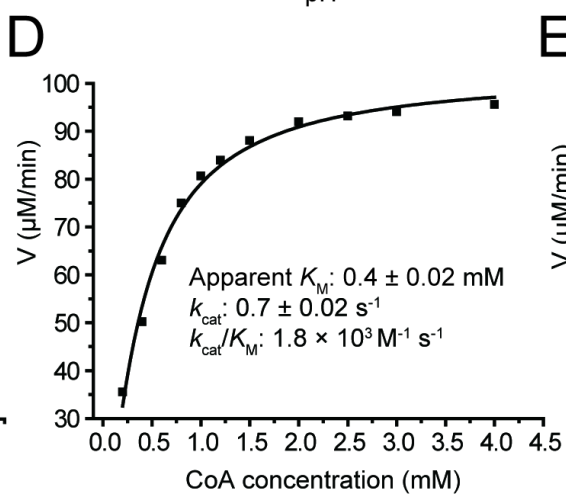
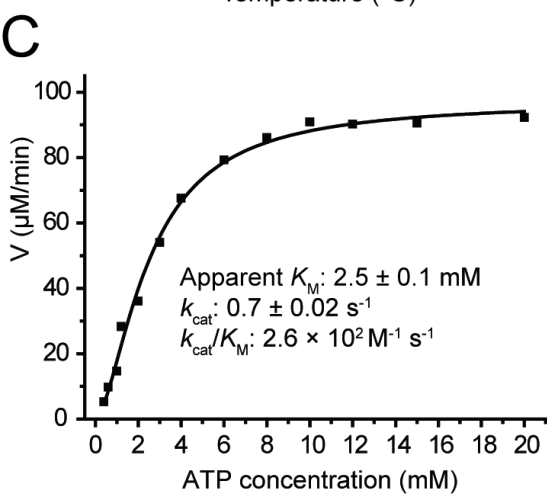
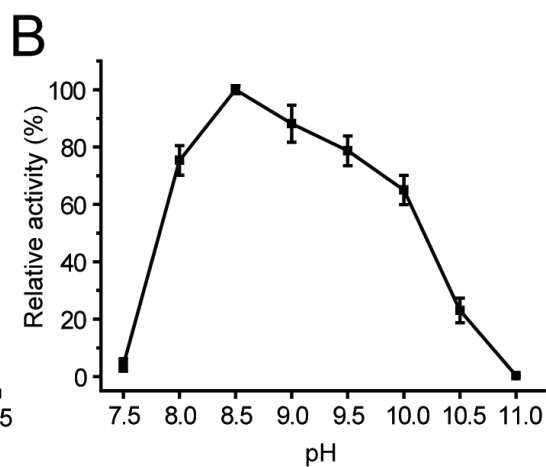
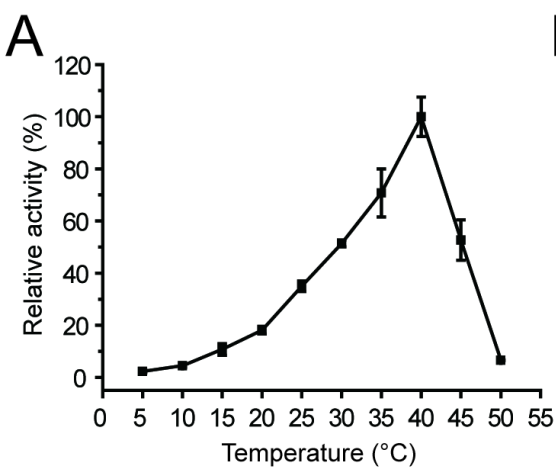
1000 bp

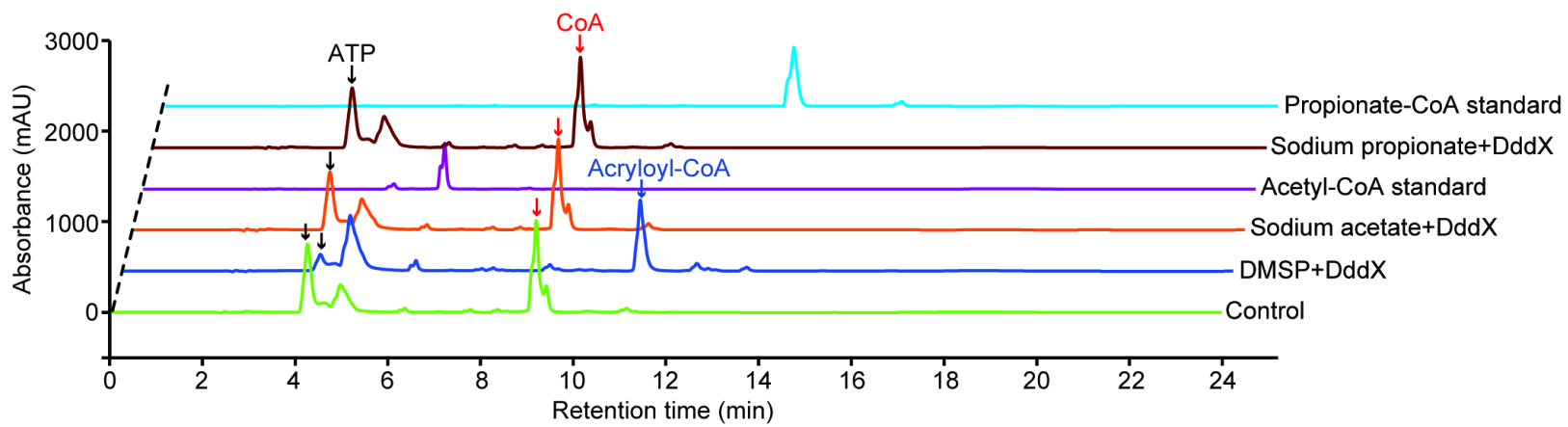
500 bp

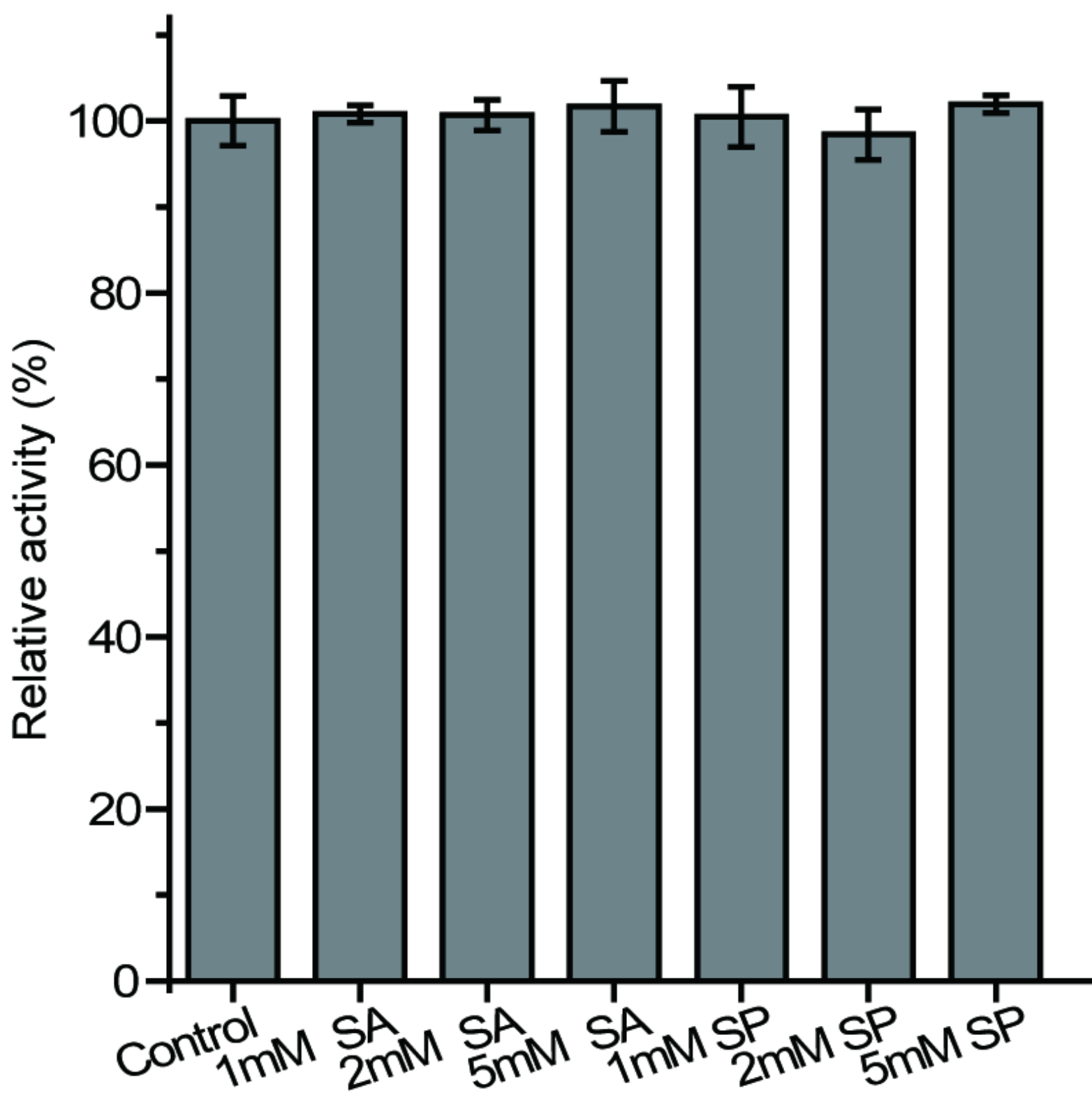


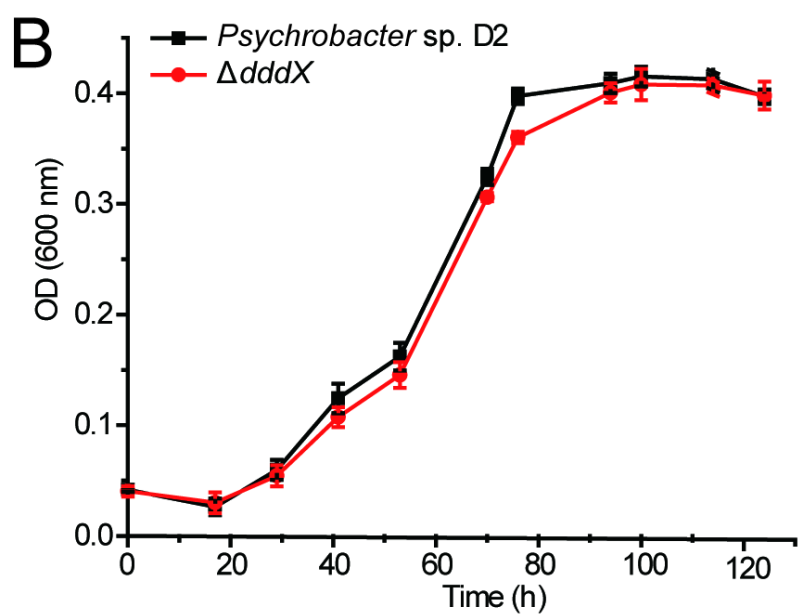
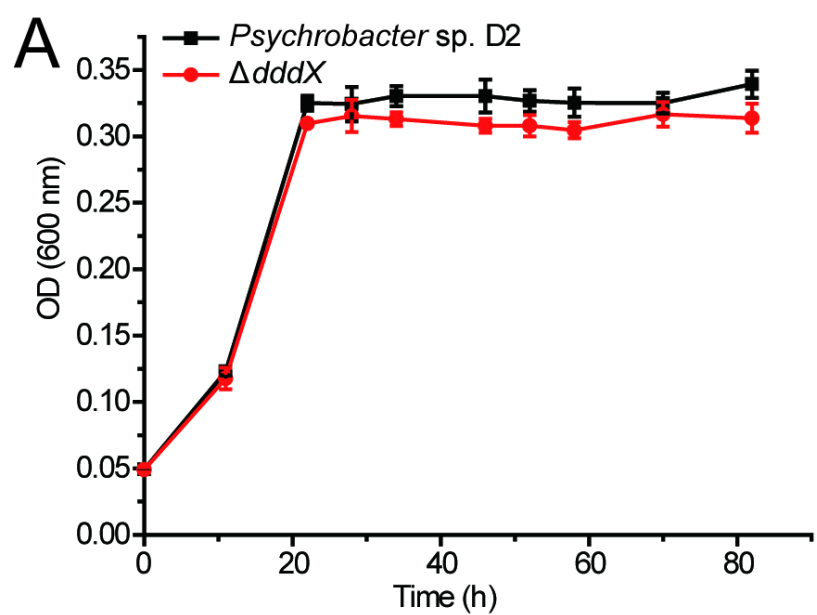


**A****B**

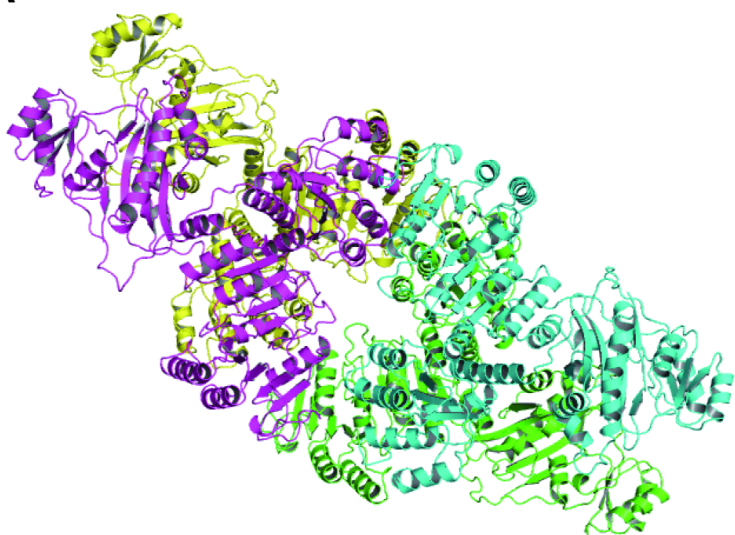




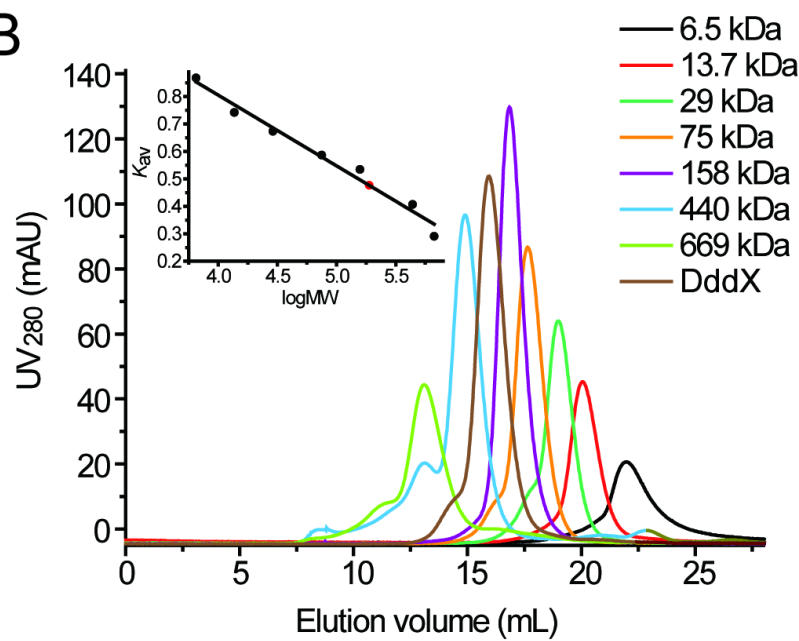




A



B



$\alpha$ -subunit

$\beta$ -subunit

